HOST MODULATORS OF THE DEATH RESPONSE TO INFLUENZA A INFECTION

APPROVED BY SUPERVISORY COMMITTEE

Michael A. White, Ph.D. (Mentor)
Beatriz M. Fontoura, Ph.D. (Chair)
Michael G. Roth, Ph.D.
Richard H. Scheuermann

DEDICATION

I would like to thank my parents for their unfailing belief in me, and their unconditional love. In addition, I would like to thank my little sister for never letting me give up. Finally, I would like to thank my mentor, Mike White, for his patience and excellent teaching.

HOST MODULATORS OF THE DEATH RESPONSE TO INFLUENZA A INFECTION

by

SAMUEL ENOCH WARD

DISSERTATION

Presented to the Faculty of the Graduate School of Biomedical Sciences

The University of Texas Southwestern Medical Center at Dallas

In Partial Fulfillment of the Requirements

For the Degree of

DOCTOR OF PHILOSOPHY

The University of Texas Southwestern Medical Center at Dallas

Dallas, Texas

May 2012

HOST MODULATORS OF THE DEATH RESPONSE TO INFLUENZA A INFECTION

Samuel Enoch Ward, Ph.D.

The University of Texas Southwestern Medical Center at Dallas, 2012

Michael A. White, Ph.D.

Influenza A virus infects 5-20% of the population annually, resulting in ~35,000 deaths and significant morbidity. Current treatments include vaccines and drugs that target viral proteins. However, both of these approaches have limitations, as vaccines require yearly development and the rapid evolution of viral proteins gives rise to drug resistance. In consequence additional intervention strategies, that target host factors required for the viral life cycle, are under investigation. Here I employed

arrayed whole-genome siRNA screening strategies to identify cell-autonomous molecular components that are subverted to support H1N1 influenza A virus infection of human mucosal epithelial cells. Integration across relevant public data sets exposed druggable gene products required for epithelial cell infection or required for viral proteins to deflect host cell suicide checkpoint activation. Pharmacological inhibition of representative targets, RGGT and CHEK1, resulted in significant protection against infection of human epithelial cells by the A/WS/33 virus. In addition, chemical inhibition of RGGT partially protected against H5N1 and the 2009 H1N1 pandemic strain. The observations reported here thus contribute to decoding vulnerabilities in the command and control networks specified by influenza virulence factors.

TABLE OF CONTENTS

PRIOR PUBLICATIONS

Gallardo TD, John GB, Shirley L, Contreas CM, Akbay EA, Haynie JM, **Ward SE**, Shidler MJ, Castrillon DH (2007) Genomewide discovery and classification of candidate ovarian fertility genes in the mouse. *Genetics* 177(1)

LIST OF FIGURES

LIST OF TABLES

LIST OF ABBREVIATIONS

HA – hemagglutinin

HBEC – human bronchial epithelial cells

IFN – interferon

MAPK – mitogen activated protein kinase

MOI – multiplicity of infection

NLS – nuclear localization signal

RISC – RNAi-induced silencing complex

RNAi – RNA interference

Chapter I: Introduction

Introduction

Influenza A

The Orthomyxoviridae family member influenza A is the causal agent of acute respiratory tract infections suffered annually by 5-20% of the human population. This infection rate results in a significant impact on morbidity, concentrated in people younger than 20 years, with economic consequences running into the billions of dollars during large epidemics [1]. Influenza infection can also result in development of chronic asthma and disease exacerbation in both children and adults. In particular, acute influenza infection can amplify airway inflammation in asthmatic patients and induce alterations in epithelial and stromal cell physiology contributing to allergen sensitization, exaggerated bronchoconstriction, and remodeling of airway epithelia [2]. Mortality rates associated with seasonal flu are low, but the aging population is at risk for development of severe congestive pneumonia which kills ~35,000 people each year in the U.S. [1]. Of continual concern is the threat of emergent high virulence strains

such as the Spanish flu (H1N1), Asian flu (H2N2) and Hong Kong flu (H3N2) pandemics which claimed millions of lives world-wide.

Current Treatment for Influenza A Infection

Current treatment for influenza A infection is focused on two main areas: vaccines and the targeting of viral proteins. However, both of these approaches are limited in their success. Vaccines require yearly development and lack the ability to protect against new strains, resulting in a lag from introduction of a new viral strain to the production of the corresponding vaccine. In contrast, drugs targeting viral proteins can show activity across a wide range of strains, but they quickly lose effectiveness due to the rapidly evolving nature of viral proteins [3]. The inherent problems with current treatment highlight the need for new drugs to combat viral infection. One therapeutic strategy currently being pursued is the targeting of host proteins required for viral replication [4]. To maximize the effectiveness of this approach, a better understanding of the host genes required for viral life cycles is needed.

Viral Replication and Life Cycle

Influenza A is a single-stranded RNA virus whose genome consists of 8 segments of negative-stranded RNA that encode for 11 functional

viral proteins [1]. To overcome the limited number of viral proteins, the virus hijacks host-cell biological systems to complete the viral life cycle of entry, replication, assembly and budding. The first step in the viral life cycle is entry into the host cell. The viral protein hemagglutinin (HA) binds to sialyated surface proteins on epithelial cells in the respiratory tract [5]. The viral particle is then taken into the cell through endocytosis. Electron micrographs show viral particles enter through coated pits, suggesting clathrin-mediated endocytosis [6]. However, viral particles are also located in smooth, uncoated invaginations [6], implying a clathrin-independent pathway as well. Furthermore, inhibition of clathrin-mediated endocytosis prevents productive infection [7]. Interestingly, infection still takes place when clathrin- and caveolin-mediated endocytosis is inhibited [7]. Studies looking at real-time entry in live cells show two-thirds of viral particles associate with clathrin-coated pits before viral entry [8].

Following entry, the virus must release its contents into the cytoplasm of the host cell. The low pH of the endosome induces a conformational change in viral HA protein, which in turn allows for the fusion of the viral particle membrane with the membrane of the endosome. At the same time, the viral protein M2, an ion channel, pumps ions into the virion, further lowering the pH. This influx of ions facilitates the release of the vRNPs into the cytoplasm of the host cell [5]. vRNPs contain nuclear

localization signals (NLS) that allow for their import into the nucleus. Once inside the nucleus, the viral RNA polymerases transcribe vRNAs.

This transcription requires the help of cellular transcription machinery, including proteins involved in RNA Poll II transcription [9]. After several rounds of transcription and protein translation, viral proteins are trafficked to the apical membrane, where new viral particles are packaged and bud off. Because of the limited number of viral proteins, this life cycle requires host cellular proteins. However, host cells have evolved measures to detect and defend against infection. One of the most potent defense mechanisms is the expression of type I interferon (IFN) genes [10]. The expression of IFNs results in the upregulation of antiviral proteins, decreased protein synthesis, and the induction of apoptosis [11,12]. The potency of IFN is illustrated by the fact that pretreatment with IFNβ protects cells from infection with virus [13]. However, influenza A has means of counteracting the cell's defenses, thus setting up a delicate interplay between host and pathogen. An example of this interplay is the activation of the mitogen-activated protein kinase (MAPK) signaling cascades. MAPKs regulate a diverse range of cellular functions, including the immune response. Not surprisingly, infection with influenza A has shown to activate several MAPK family members [14-16]. One of these, the JNK subgroup, is activated upon productive infection by accumulating

viral RNAs [15]. This activation is important in regulating the expression of IFNβ [10]. The importance of the activation of JNK is seen as inhibition of JNK results in enhanced viral production [15]. In contrast, the activation of the MEK/ERK cascade is beneficial for virus, as seen by the fact that inhibition of this pathway impairs viral growth [16,17].

Another example of the interplay between host and pathogen response is the activation of the NF-κB pathway. NF-κB is a family of transcription factors that regulate more than 150 genes [18], including several anti-viral proteins such as IFNβ and TNF-α [18]. NF-κB is activated upon influenza A infection and was originally thought to be a major inducer of the antiviral state [19], as it is in other RNA viruses [20]. However, in the case of influenza A, NF-κB seems to have a supportive role in viral infection. This was demonstrated in two studies where pre-activation of NF-κB resulted in higher levels of viral replication. Conversely, inhibition of NF-κB resulted in decreased viral titers [21,22]. Indeed, pharmacological inhibitors of NF-κB have antiviral activity *in vivo* [4]. Thus it appears that influenza A has subverted what is normally an antiviral response to support its own life cycle.

One of the major ways that influenza A is able to avoid the immune response is through the actions of the viral protein NS1. NS1 is able to control the immune response by regulating IFN signaling, impairing mRNA

processing and export, which results in global inhibition of gene expression, and by inhibiting innate immunity effectors [23-26]. NS1 inhibits IFN production by regulating the activation of IRF3 and NF-κB as well as inhibiting the function of RIG-I [23-26]. It also binds and sequesters dsRNA, thus preventing the detection and activation of the antiviral protein PKR [23-26]. The importance of NS1 in the control of the immune response is seen as viruses lacking the NS1 protein induce a greater IFN response, thereby inhibiting viral replication [23-26]. Another important aspect of NS1 is its ability to delay the onset of apoptosis [27,28].

Death Response to Infection

Apoptosis is a defined form of cell death that plays a role in virus infections [29]. Its role in viral infection is typically thought to be a host cell defense because many viruses have proteins that inhibit apoptosis. It has long been known that infection with influenza A induces apoptosis [30-33]. However, the result of this induction, in regards to viral outcome, is still unclear. Several things argue for it having an antiviral role. For example, influenza A virus, when lacking the viral protein NS1, is a stronger inducer of apoptosis than wild type virus [27]. Additionally, activated caspases can cleave the viral NP protein, preventing it from being packaged into

viral particles [34]. These observations would suggest that apoptosis has an antiviral function in cells. However, in the presence of caspase inhibitors, viral propagation is strongly inhibited [35]. This appears to be a result of vRNPs being retained in the nucleus [35]. Also, as mentioned before, NF-κB has both pro- and anti-viral functions. The pro-viral function has been linked with its pro-apoptotic activity [22]. This is consistent with an early report that overexpression of the anti-apoptotic protein, BCL-2, results in vRNP nuclear retention and lower viral titers [36,37], as well as reports that showed inhibition of apoptosis inhibited viral replication [38-40]. Taken together, these observations would imply that the cell mounts an anti-viral response that includes the induction of apoptosis. In turn, the virus limits, but does not abolish, this response and uses it to support viral replication. This places the control of apoptosis as one of the key balancing points in the outcome of influenza A infection. It has both pro-viral and anti-viral activity. If the control of apoptosis could be returned to the cell, it would then act in an anti-viral fashion and inhibit viral production, suggesting a novel therapeutic strategy. One study that supports this idea is a recent study done in duck cells. Waterfowl, including ducks, are a natural host for influenza A. Interestingly, ducks infected with influenza A do not present any pathological symptoms [41]. However, chickens infected with the same strain show significant

symptoms that often lead to death [1, 41]. To understand the difference in response on a cellular level, primary lung cells were cultured from both ducks and chickens. When infected with influenza A, the duck cells showed a rapid onset of apoptosis, whereas the chicken cells had a delayed response. Interestingly, when duck cells were infected with a strain that causes pathological symptoms, the apoptotic response was slowed to that of the chicken cells [41]. These observations imply the possibility that in duck cells, the apoptotic response has anti-viral activity, thereby removing the pathological response to viral infection *in vivo*. This suggests a novel therapeutic approach to treating influenza A. If one could change the balance of the apoptotic response so that it acts in an anti-viral way, one could effectively treat influenza A. To accomplish this strategy, it would be beneficial to have a better understanding of the host factors involved in modulating cell death in response to influenza A infection.

Genome-wide siRNA Screening

The arrival of genome-wide siRNA libraries, combined with the ability to target different oligos to individual wells within a 96-well plate has given rise to the ability to perform high throughput siRNA screens. Indeed, high throughput screens have been used with great success to

explore the functional genomics of many biological processes [42]. The breadth of coverage and the unbiased nature of this approach make it especially inviting as a tool for the discovery of novel drug targets.

The power of siRNA screens, combined with the ease of detecting cell viability, allow for the creation of a strategy to identify novel host modulators of cell death (Figure 1.1). Here I present the results of this strategy, which has resulted in the identification of 235 candidate modulators, many of which have not been previously identified as players in the host-pathogen interaction. Potential mechanisms were explored with direct follow-up of a selected panel as well as leverage of existing biological data. I have also confirmed with pharmacological experiments that the pathways identified in the screen have therapeutic potential.

Figures

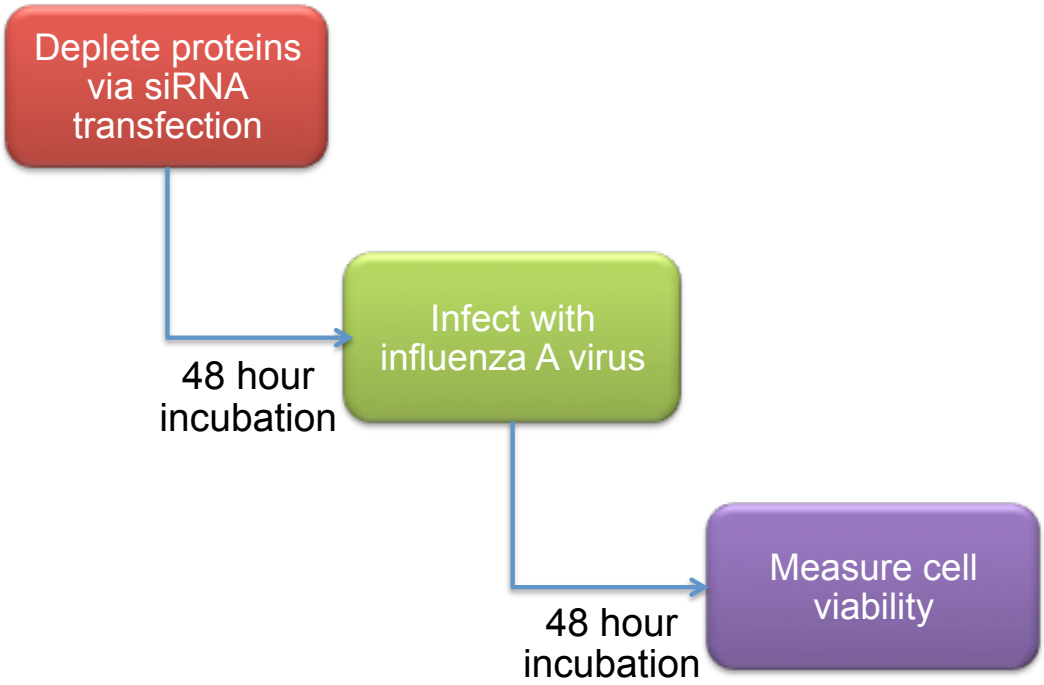

Figure 1.1. Strategy for Identification of Death Modulators

To identify host modulators of the death response, HBECs will be transfected with siRNA followed by a 48-hour incubation period, allowing for target depletion. Cells will then be infected with influenza A virus and cell viability will be measured 48 hours post-infection.

CHAPTER II: IDENTIFICATION OF HOST MODULATORS OF INFLUENZA A INFECTION

Introduction

A better understanding of the host pathways involved in the death response to influenza A would facilitate the development of novel therapeutic treatment. The creation of siRNA genome-wide libraries provides a tool to generate an unbiased experimental platform to identify host modulators of viral infection. siRNAs use the RNA interference (RNAi) pathway to regulate protein levels in cells [43]. RNAi uses double stranded RNA precursors. In the case of siRNA, Dicer processes double stranded RNA precursors into 21-25 nucleotide strands [44,45]. Processed siRNAs are then loaded into the RNAi-induced silencing complex (RISC), where they promote sequence-specific degradation of target mRNAs, mediated by Argonaute 2 [46,47]. The ability of siRNAs to deplete mRNAs makes them a useful tool in dissecting functional genomics. They can be designed to target a gene of interest, are deliverable in cell culture, and can be produced on a large scale. However, siRNAs have some drawbacks as well. The depletion of mRNA is transient, and results vary depending on the protein targeted and the

cell type used [48]. mRNA depletion is not always complete, and residual protein can have enough activity to prevent a phenotype. Finally, siRNAs can have off-target effects, giving rise to a false positive result [49]. Despite these drawbacks, genome-wide siRNA screening has been shown to successfully provide an unbiased approach for identifying novel biological pathways and therapeutic targets [42]. A key to leveraging this tool is to design the screen to maximize the information obtained and, at the same time, limit the noise. To this end, I designed a screening strategy that would be physiologically relevant, had an end point assay amenable to high-throughput screening, and produced robust phenotypes. Here I discuss the optimization and execution of this screening strategy that resulted in the identification of modulators of the host response to influenza A infection.

Results

Optimization of the Screen

The object of this project is to identify targets that have therapeutic potential in treating influenza A infection; however, the response to infection is different depending on the cell type. This point is illustrated *in vivo* where macrophages and dendritic cells have very different responses

to influenza A infection. Macrophages undergo apoptosis within 36 hours, whereas dendritic cells remain viable 48 hours post-infection [50]. This example illustrates the importance of selecting a physiologically relevant cell type. The pathology of influenza A includes changes throughout the respiratory tract; however, the major site of impact is the respiratory epithelia, as seen by bronchoscopy of patients with uncomplicated influenza infections, with viral antigen found mainly in the epithelial cells and mononuclear cells [1]. For this reason, I chose to use telomerase-immortalized human bronchial epithelial cells (HBECs), specifically HBEC30-KT cells. These cells retain the ability to differentiate into a polarized ciliated epithelial sheet [51], adding to their physiologic relevance.

The first step in optimizing the screen was to characterize the response of HBECs to influenza A infection. HBECs exposed to a range of viral titers showed a striking ability to resist propagation of plaques as compared to MDCK cells, a viral permissive cell line. However, examination of infected HBECs revealed a decrease in cellularity in the plaques (Figure 2.1) and implied infection-dependent cell death. Consistent with this finding was the fact that viral protein was detectable by both western blot and immunofluorescence with near 100% of cells infected after 24 hours using a multiplicity of infection (MOI) of 5 (Figure

2.2). This infection rate leads to a fifty percent decrease in cell viability at 48 hours post-infection, as measured by the CellTiter-Glo assay, which correlates cell viability with detection of ATP levels (Figure 2.3). HBECs were tested with a range of MOIs for cell viability showing a dose-dependent response (Figure 2.3). Interestingly, this dose-dependent response was not linear. This is likely a result of asynchrony in infection times, caused by cell cycle differences as well as the 96-well plate format. Despite the asynchrony, the cell viability was consistent within experiments and had a high level of reproducibility. To identify modulators of the death response in both directions, I chose a 48-hour exposure with an MOI of 5 as the end point for the screen. Another reason for selecting this concentration is that we are dealing with a single cycle infection, as evidenced by the near 100% infection rate 24 hours post-infection (Figure 2.2).

These observations allowed for the adoption of a screening strategy consisting of 48-hour incubation post siRNA transfection, followed by a 48-hour exposure to influenza A/WSN/33 (WSN) or carrier, with cell viability as the endpoint assay (Figure 1.1). Screening was done in a two-condition biological triplicate. Each siRNA pool was transfected into six plates: three for virus-infected and three for mock-infected conditions. Transfection was performed with high-throughput equipment. The use of

high-throughput equipment can result in positional artifacts. A scatterplot analysis of the screening data identified a row-dependent position effect. This makes it difficult to compare cell viability from row to row, as some rows are artificially high while others are artificially low. However, values in rows were internally consistent. This was evidenced by the fact that siRNA oligos, when tested in multiple rows, retained their relative values. To remove this position effect, each well was normalized to the row median well. Subsequent scatterplot analysis confirmed the effectiveness of this method to remove position effects. However, the use of normalized ratios to determine cell viability gives extra weight to oligos that increase cell viability. For this reason, values were log2 transformed to give a more accurate weight distribution. Using day-specific variance numbers, z-scores were calculated, thus leveraging the data set as an internal negative control. A z-score ratio was then made from the z-scores of virus-treated versus mock-treated HBECs, allowing for the comparison of experiments done on separate days (Figure 2.4).

Using an arbitrary cutoff for siRNA pools with z-scores that were equal to or greater than 3 standard deviations above, termed *resistors*, or below, termed *sensitizers*, the mean of the population. The screen identified 220 candidate hits. To this list I added another 15 siRNA pools

based on z-scores and viral interactions for a total of 235 candidate hits: 53 resistors and 182 sensitizers (Table 2.1).

Terminology of Hits

In this study I will be using the following terminology to describe the results of the initial screen: *resistor* and *sensitizer*. The term *resistor* refers to siRNAs that increase cell viability upon exposure to virus. The term *sensitizer* refers to siRNAs that decrease cell viability upon exposure to virus. Cell viability was measured as the normalized ratio of virus-infected cells over mock-infected cells. Thus, resistors show a relative increase in cell viability and sensitizers show a relative decrease in cell viability. It is important to note that these terms refer to the siRNAs and not the genes associated with them. For example, when I say that COPB2 is a sensitizer, I mean that the siRNA oligos targeting COPB2 decrease the relative viability of cells exposed to virus. It does not mean that the COPB2 gene sensitizes cells to viral infection, but it is simply a description of the phenotype of the siRNA oligos. The implication of these phenotypes will be discussed in further detail later.

Reproducibility

To confirm that the results of the screen were robust, I selected a panel of siRNAs with a range of z-scores for retesting. Retesting was conducted

with 163 siRNAs: 126 resistors and 37 sensitizers. Experimental conditions were kept the same as the original screen. Each oligo was tested in triplicate and compared to control siRNA. The reproducibility of the phenotype was analyzed using a student TTest with the following results: seventy-eight percent of resistors, and ninety-five percent of sensitizers showed significant reproducibility (Figure 2.5).

Off-Target Effects

Another caveat of screening is the potential for off-target effects from the siRNAs to produce false positives. One way to look at off-target effects is to test for reproducibility of a phenotype with several different oligos that target the same protein. If the phenotype is real, it should be reproducible with multiple oligos. To look at the contribution of off-target effects to our data, 88 siRNAs were tested with 4 individual oligos. Fifty-eight percent of tested oligos showed reproducible phenotypes with two or more oligos. It is important to note that the lack of reproducibility of a phenotype with two or more oligos does not mean there is an off-target effect. It does, however, lessen the confidence in the hit.

Discussion

Influenza A needs many cellular proteins and pathways to complete its viral life cycle. One pathway that is vital in deciding the outcome of infection is the death response upon infection with virus. In this chapter, I have shown the identification of host modulators of the death response to influenza A infection. This was done in an immortalized human bronchial epithelial cell line. The choice of this cell line is important, as it represents a physiologically relevant cell for both infection conditions and cell death mechanisms. Many studies in influenza have been done with cancer cells, which often have an altered death response. This altered death response would decrease their value as a physiological relevant model for influenza A infection. HBECs also have the ability to fight against viral infection, as evidenced by the low levels of viral titers and subsequent plaque formation. This makes these cells good candidates to identify the innate immunity genes that actively fight against viral infection *in vivo.*

The initial screen identified two types of modulators of cell death, which I have termed resistors and sensitizers. Resistors are siRNAs that, when depleted, deflect death upon infection with influenza A virus. Sensitizers are siRNAs that, when depleted, increase death. These results were highly reproducible, strengthening the belief that the screen can accurately identify modulators of the death response. Unfortunately, when tested with single siRNA oligos, the results were not as

reproducible. This could mean there is a significant contribution of off-target effects. However, the lack of reproducibility could also be a result of the change in format. In the large screen, the use of robotic equipment and large number of internal controls increased the consistency of the screen. The retests were done in a smaller format with fewer negative controls, thereby increasing the standard deviation. The change in format also decreased the consistency between experiments, thus adding to the lack of reproducibility. Another thing that strengthens the confidence in the screen is the pulling out of proteins known to be involved with the viral life cycle and/or to interact with viral proteins, including two PI3K regulatory proteins. PI3K is known to be involved in viral entry as well as the death response to viral infection [28,52,53]. The strongest hits in this pathway were resistors. However, the screen also identified weak sensitizers involved in PI3K signaling. It would be interesting to see if the different phenotypes correlated with different roles in viral infection. Also identified were members of the vacuolar ATPase, which are appear to be involved in virus membrane fusion in late endosomes [54], as well as SFPQ, a splicing factor that interacts with the viral polymerase [55]. The screen did not pull out all proteins known to be involved in viral infection. These seemingly false negatives could arise for several reasons: they could be a result of insufficient protein depletion by siRNA, cell-type

specific requirements, protein redundancy, single cycle infection, or influenza strain specific requirements.

The separation of hits into resistors and sensitizers is a good starting point. However, it tells little about the resulting effect on the outcome of infection. Cells could deflect death because they prevent viral entry or replication, or they could prevent the cells apoptotic response to viral infection. They could also enhance death as a result of deflecting the virus's ability to stop the cells innate immune response or by increasing the rate of infection. Understanding these outcomes would help to identify therapeutic targets; therefore, a more functional classification of hits would be beneficial toward the discovery of new drug targets.

Materials and Methods

Cell Culture

HBEC30-KT cells were a gift from Dr. Minna and were cultured in KSFM (invitrogen Cat#17005) with 1% pen/strep antibiotics. MDCK cells were grown in DMEM with 10% FBS.

Plaque Assay

MDCK and HBEC-30KT cells were plated in 6-well plates and left overnight. Cells were infected with WSN virus at 10-fold dilutions with a starting concentration of 10^8 pfu/ml. Infected cells were allowed to

incubate at 37^{o}C with tilting every 10 minutes. After one-hour incubation, liquid was aspirated and 2 ml of agar solution was added to wells and allowed to solidify for 1 min. Plates were incubated for 48 hours at 37^{o}C. Following incubation, plates were fixed with formaldehyde for one hour. Fixative and agar were removed and cells were stained with crystal violet. (Experiment performed by Pei-Ling Tsai of the Fontoura lab)

Viral Protein Detection

HBECs were plated in 96-well at 20,000 cells per well and incubated overnight. Cells were infected with WSN virus at an MOI 5. Whole cell lysates were collected at 6, 12, or 24 hours post-infection and lysates were run on a 12% SDS-PAGE gel and transferred to a nitrocellulose membrane. Plates for immunofluorescence were fixed with 4% formaldehyde at 6, 12, or 24 hours post-infection. Viral protein was detected with antibodies for pan influenza A (1:200) (western blots), M2 (1:500) or NP (1:500) proteins followed by either detection with HRP conjugated secondary or staining with Alexa 498 (1:5,000) or Alexa 594 (1:5,000) conjugated secondary antibodies. Wells were imaged with a 20x lens on a BD Pathway 855 microscope.

Cell Viability Assay

To test for cell viability, 15µl of Promega's CellTiter-Glo was added to wells on a 96-well plate for a final concentration of 7.5%. Plates were

rocked for two minutes followed by 10 minutes incubation. Luciferase activity was measured on a PerkinElmer EnVision reader.

siRNA Screen

The siRNA screen was performed using the Dharmacon library targeting 21,125 genes. HBECs were plated into 96-well plates at 10,000 cells per well and siRNAs were reverse transfected. Each siRNA pool was transfected in two sets of triplicates for a total of 6 wells for each siRNA: 3 wells for infection with influenza A and 3 wells for mock infection, with a concentration of 50nM of siRNA oligos and 0.1% DharmaFECT 3 reagent. To increase consistency, siRNA pools were added to 96-well plates using the BioMek robot. Cells and transfection reagents were added with a multidrop dispenser. Cells were incubated for 48 hours after transfection and infected with influenza A A/WSN/33/H1/N1 (WSN) at an MOI of 5. Forty-eight hours after infection, cell viability was assayed as described above.

Data Normalization and Z-score Calculation

To remove position effects, raw data numbers from each well were normalized to the median well of their respective row. Normalized data was log2 transformed for a more accurate distribution of sensitizers and resistors. Relative cell viability was measured by taking the ratio of virus-infected cells over mock-infected cells. To allow for comparison between

experimental days, z-scores were calculated for each siRNA pool where Z=(Ratio – day-specific mean ratio)/day-specific standard deviation. To control for contamination and technical issues, the top 5% of outliers with the highest coefficient of variation among triplicates were removed.

Figures

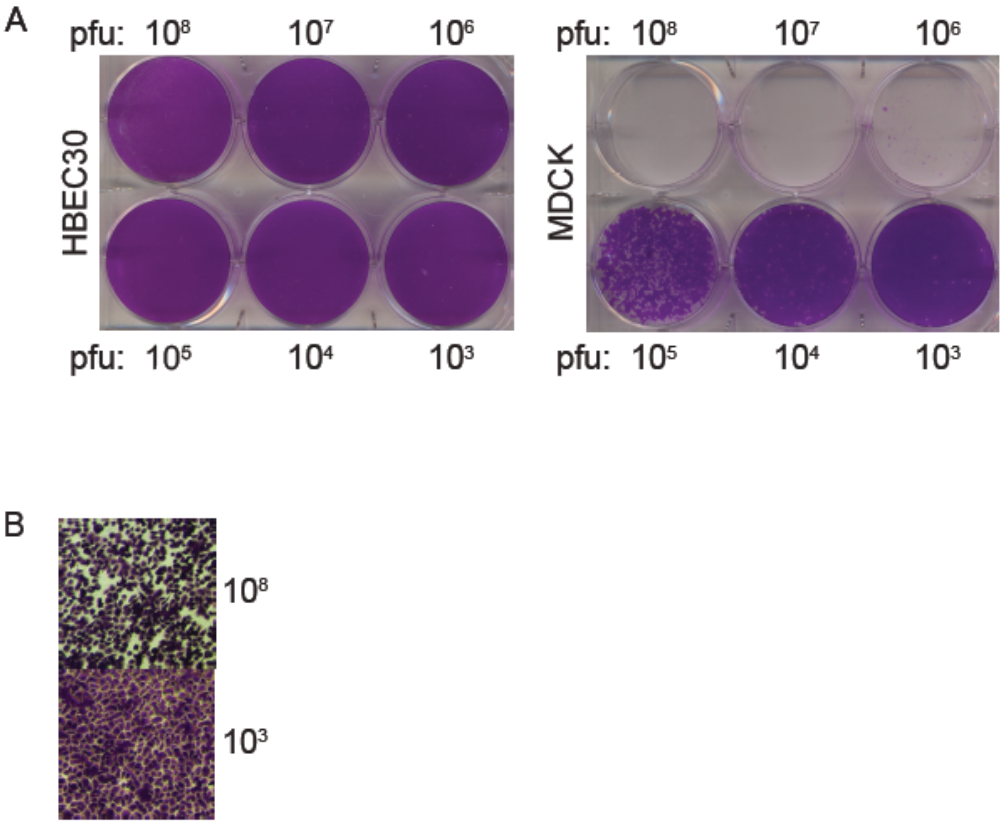

Figure 2.1. HBEC Response to Influenza A

(A) A/WSN/33/H1/N1 (WSN) plaque-formation was assayed in HBEC30 and MDCK cells using the indicated viral titers.

(B) 4x magnified images of crystal violet stained monolayers.

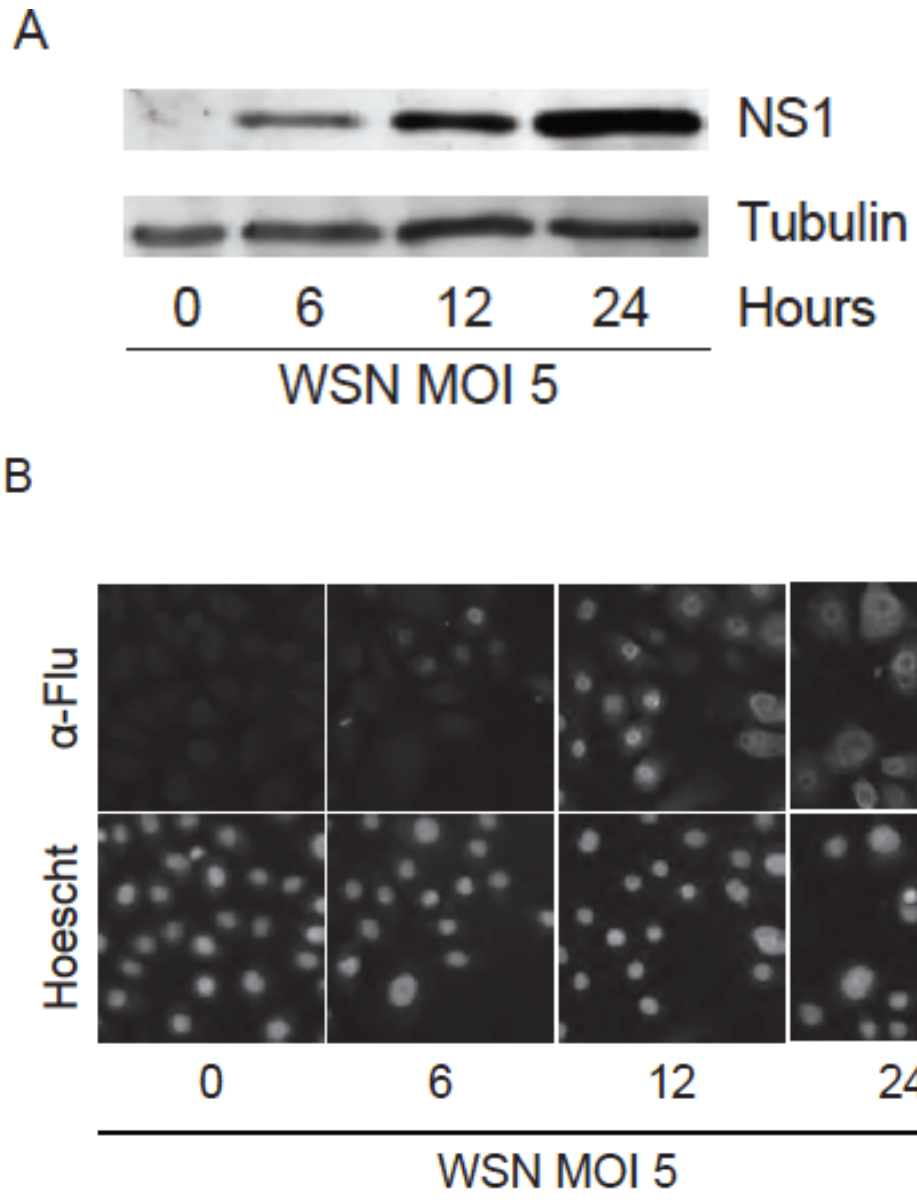
A
NS1
Tubulin
0
6
12
24
Hours
WSN MOI 5
B
α-Flu
Hoescht
0
6
12
24 hrs
WSN MOI 5

Figure 2.2 Viral Replication in HBECs

(A) HBEC30s were infected with WSN at an MOI of 5 and examined for accumulation of viral proteins by immunoblot at the indicated time-points post-infection. (B) Cells treated as in A were immunostained for detection of viral protein accumulation at single cell resolution. Top panels labeled α-Flu show anti-influenza A staining and bottom panels labeled Hoescht show nuclear staining with Hoescht.

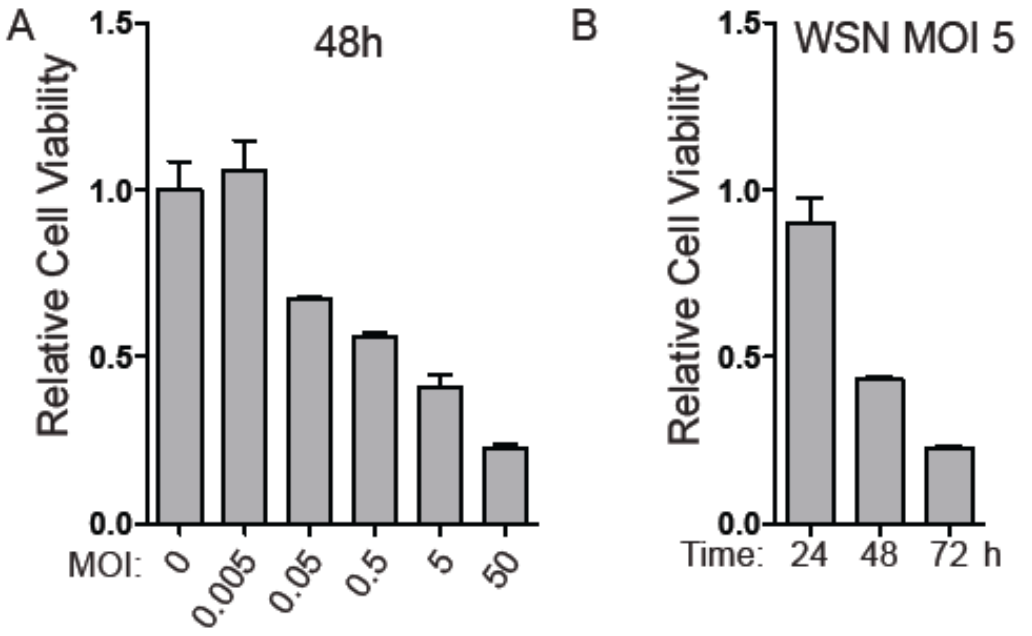

Figure 2.3 HBEC Death Response to WSN Infection

(A) HBECs were infected with WSN at varying MOIs and cell viability was measured at 48-hours post-infection. HBECs show a dose-dependent death response to infection. (B) HBECs were infected with an MOI of 5 and cell viability was measured at varying time points. A 48-hour infection at an MOI of 5 results in approximately 50% cell viability.

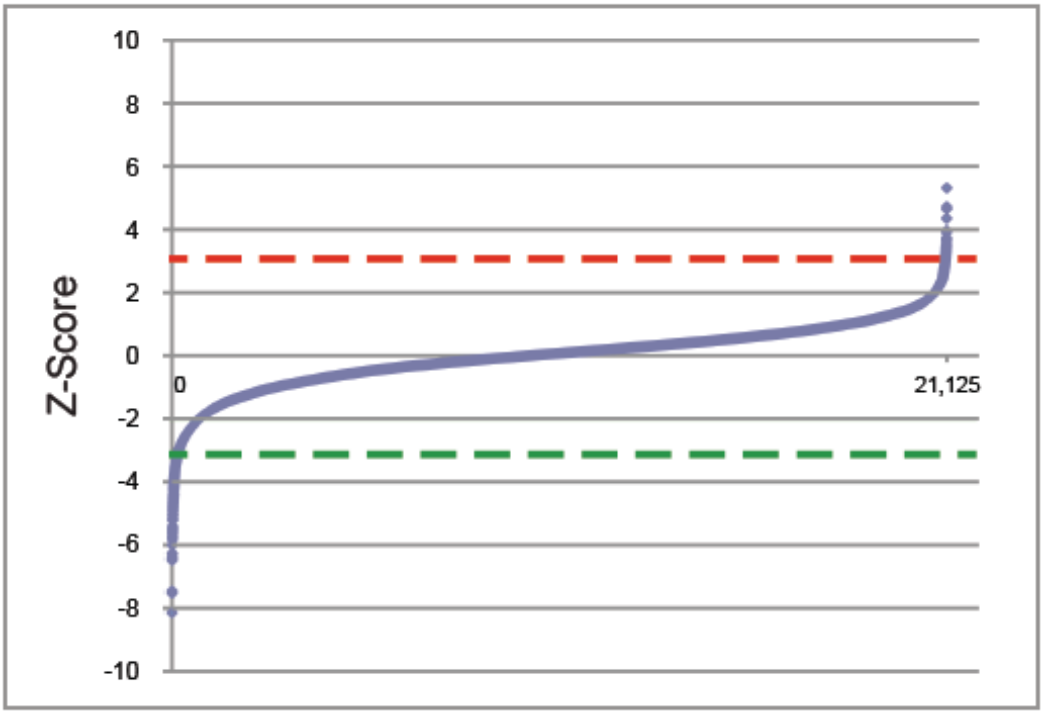

Figure 2.4 Screen Results

The rank-ordered z-score distribution from each of 21,125 siRNA pools targeting the annotated human genome is shown. Dashed lines indicate 3 standard deviations above (red) and below (green) the mean of the distribution.

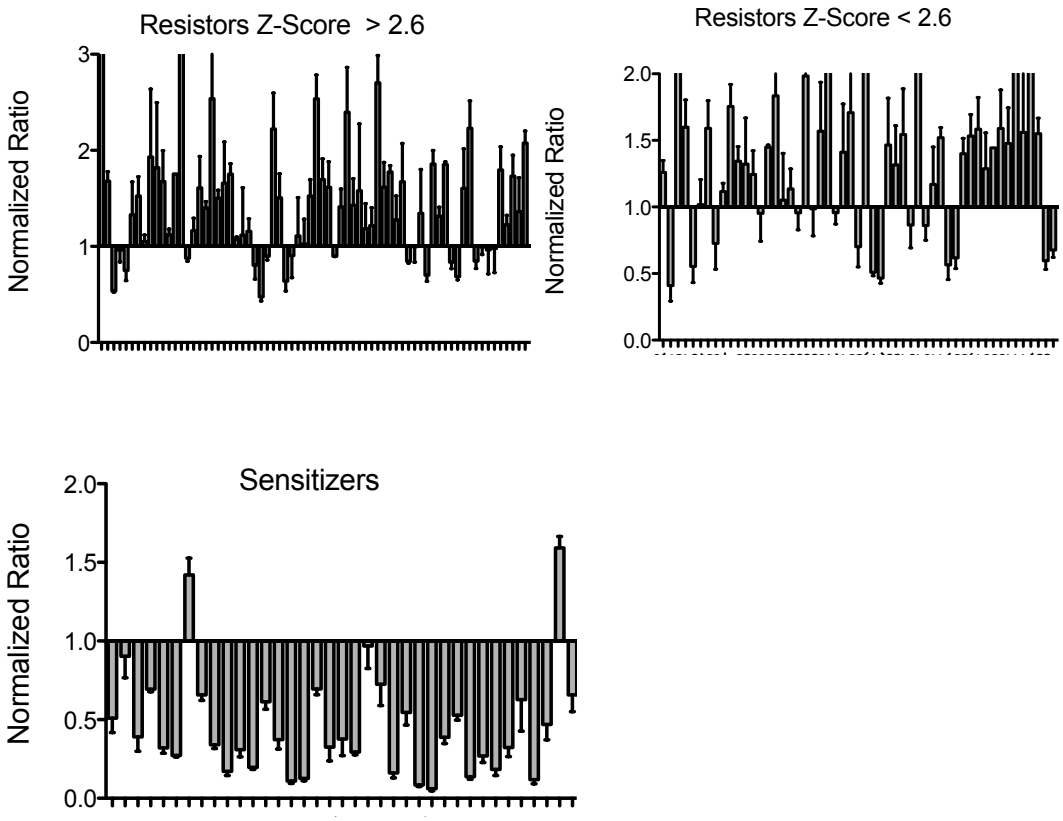

Figure 2.5. Reproducibility of Screen

A panel of 163 genes (126 resistors and 37 sensitizers) were tested for reproducibility. siRNA pools are plotted from left to right according to original z-scores. Relative cell viability is plotted on the Y-axis. Phenotypes showed significant reproducibility with 81% of tested siRNA pools reproducing the original phenotype.

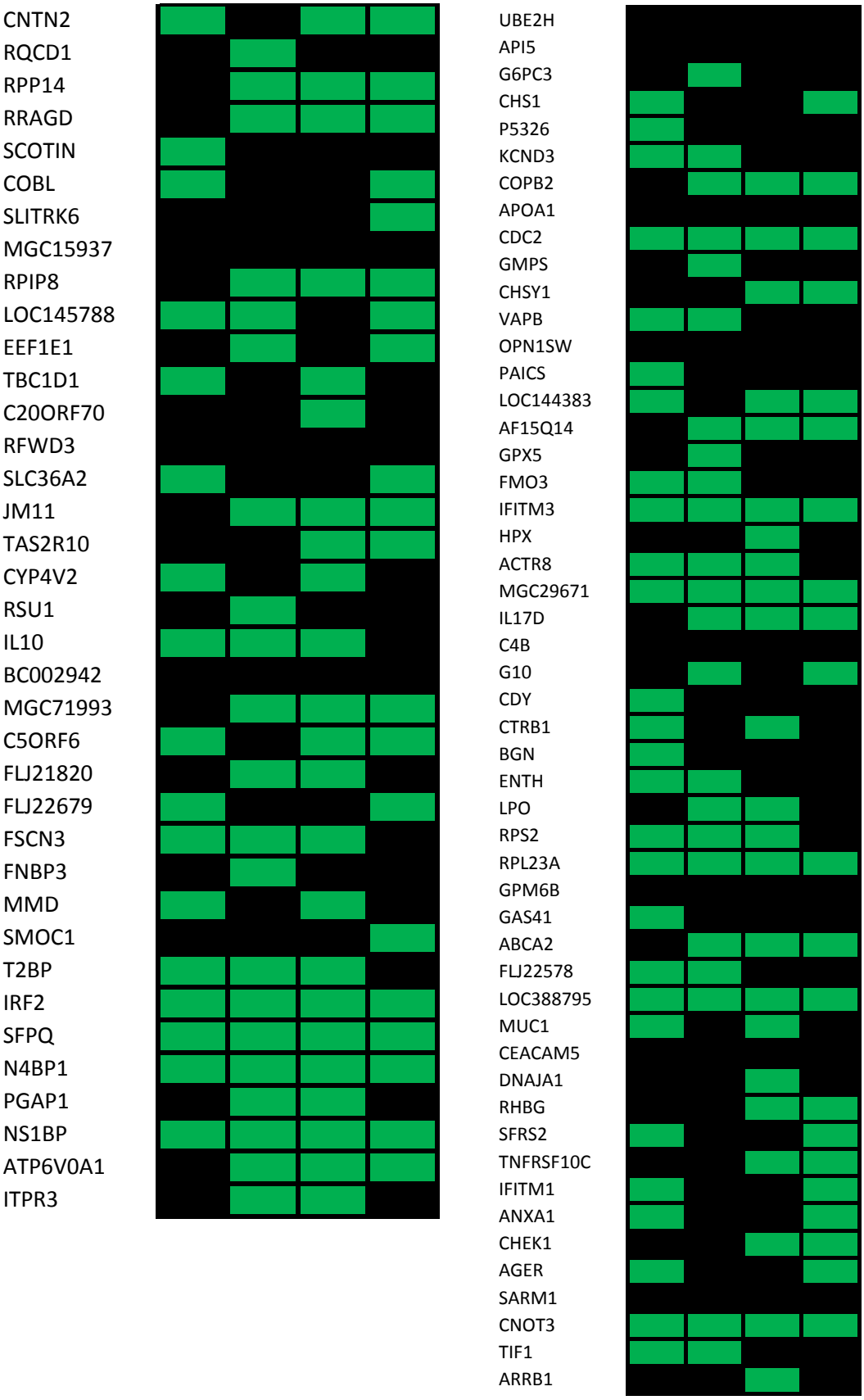
CNTN2
RQCD1
RPP14
RRAGD
SCOTIN
COBL
SLITRK6
MGC15937
RPIP8
LOC145788
EEF1E1
TBC1D1
C20ORF70
RFWD3
SLC36A2
JM11
TAS2R10
CYP4V2
RSU1
IL10
BC002942
MGC71993
C5ORF6
FLJ21820
FLJ22679
FSCN3
FNBP3
MMD
SMOC1
T2BP
IRF2
SFPQ
N4BP1
PGAP1
NS1BP
ATP6V0A1
ITPR3
UBE2H
API5
G6PC3
CHS1
P5326
KCND3
COPB2
APOA1
CDC2
GMPS
CHSY1
VAPB
OPN1SW
PAICS
LOC144383
AF15Q14
GPX5
FMO3
IFITM3
HPX
ACTR8
MGC29671
IL17D
C4B
G10
CDY
CTRB1
BGN
ENTH
LPO
RPS2
RPL23A
GPM6B
GAS41
ABCA2
FLJ22578
LOC388795
MUC1
CEACAM5
DNAJA1
RHBG
SFRS2
TNFRSF10C
IFITM1
ANXA1
CHEK1
AGER
SARM1
CNOT3
TIF1
ARRB1

Figure 2.6 Off-target Tests

To test for the contribution of off-target effects, 88 candidate siRNAs pools were tested as four individual oligos and a TTest was performed to measure significance. Resistors are plotted in the left group and sensitizers on the right. Green boxes indicate p values < 0.05. Approximately 60% of tested siRNAs reproduced with 2 or more oligos.

Table 2.1 Candidate Hits Resistors				
ACAP2	FAM53C	LOC389749	RPGRIP1	TAS2R10
ANKFY1	FSCN3	N4BP1	RPP14	TBC1D1
ATP6V0A1	GLYATL1	PCTK3	RQCD1	TIFA
C20orf70	IL10	PFTK1	RRAGD	TMEM164
C2orf43	ING2	PGAP1	RSU1	TROAP
C4orf23	IRF2	PIK3R3	RUNDC3A	ULBP2
CCDC120	IVNS1ABP	PIK3R4	SFPQ	VPS4B
CNTN2	LMF2	PPP1R3B	SHISA5	VTA1
COBL	LOC121792	RFWD3	SLC36A2	ZRANB1
CYP4V2	LOC145788	RNASEK	SLITRK6	
EEF1E1	LOC388476	RNASEL	TARBP1	

Table 2.2 Candidate Hits Sensitizers							
ABCA2	CASC5	EIF4G2	IFT122	LOC400652	PAICS	SHPK	ZMYM6
ACTB	CCAR1	EVL	IGDCC3	LOC401394	PCF11	SIRT3	ZNF184
ACTR8	CCDC117	FAM166A	IL17D	LOC401544	PLCXD2	SLC1A4	ZNF407
ADORA3	CCS	FAM174A	ING2	LOC401923	POLE	SLC22A23	ZNF580
ANGEL1	CDC2	FANCI	INTS6	LOC402582	POLR2D	SLC5A1	ZNF584
ANKRD57	CDKL5	FKBP1A	ISOC2	LPO	PRL	SMARCD2	ZNF678
ANLN	CDY1	FLJ41327	ITGAE	LRRC17	PRRT3	SOLH	ZNF80
ANXA1	CEACAM5	FMO3	KCND3	LYPLA2	PTGFRN	SPNS3	
AP1M1	CHCHD5	FZD6	KCTD18	LYST	PYCR2	SYT8	
AP1S2	CHEK1	G6PC3	LGALS3BP	MANEAL	RGS18	TAC1	
API5	CHSY1	GLB1L2	LOC144383	MCART1	RGS4	TCF25	
APOA1	CLINT1	GMPS	LOC145767	MKRNP5	RHAG	TEKT4	
ATP5A1	COBLL1	GP1BB	LOC146053	MRM1	RHBG	TMCO6	
BAT2	COPB2	GPAA1	LOC220906	MRPL48	RNF213	TMEM216	
BGN	COX6A2	GPM6B	LOC338799	MUC1	RPL18A	TMEM45B	
BUD31	CTRB1	GPN2	LOC341098	MYRIP	RPL23A	TNFRSF10C	
C10orf68	CYLC1	GPR162	LOC387832	NAPA	RPL27	TRAPPC10	
C11orf68	DCAKD	GPX5	LOC388401	NAT14	RPL35	TRRAP	
C12orf47	DDX46	GTF3A	LOC388519	NCR3	RPS2	TXNRD2	
C13orf29	DHX40	HNRNPAB	LOC388532	NDUFV1	RPS28	UBE2H	
C20orf200	DIRC2	HPX	LOC388923	NTSR2	RPS29	UIMC1	
C21ORF93	DNAJA1	HTR3E	LOC389295	NUMB	SCO2	VAPB	
C4B	DNAJC5B	HUMRTVLH3	LOC389425	NUP85	SCPEP1	WDR6	
C6orf184	DOCK5	IFITM1	LOC389685	OPN1SW	SELENBP1	YEATS4	
C9ORF23	EFCAB8	IFITM3	LOC390547	OVOL2	SFRS2	ZBTB45	

CHAPTER III: FUNCTIONAL CLASSIFICATION AND DATA INTEGRATION FOR MECHANISTIC UNDERSTANDING OF CANDIDATE HITS

Introduction

The genome-wide siRNA screen identified gene depletions that either deflected or promoted bronchial epithelial cell death upon exposure to influenza A, but did not look at the outcome of viral replication. An understanding of how these candidate hits affect viral replication would yield insights into potential mechanisms behind the death response. With that information, candidate hits can be parsed into four functional classes: 1) Targets that, when depleted, enhance bronchial epithelial cell survival upon exposure to H1N1 and are required for viral replication. This class presumably represents host factors that facilitate viral infection and/or are required to support viral replication. 2) Targets that, when depleted, reduce bronchial epithelial cell survival upon exposure to H1N1 and are required for viral replication. This important and initially unanticipated class likely represents proviral host factors that deflect cell death checkpoint responses that would otherwise be induced upon viral infection. 3) Targets that, when depleted, reduce bronchial epithelial cell survival upon exposure to H1N1 and enhance viral replication relative to controls.

Recently discovered innate immune pathway components, such as IFITM3, that are responsive to H1N1 infection are members of this class, which likely represent antiviral factors that oppose infection. 4) Targets that, when depleted, enhance bronchial epithelial cell survival upon H1N1 exposure and enhance viral replication as compared to controls. To separate hits, a panel of genes was selected for direct follow-up. I also integrated orthogonal data sets that describe host gene function in regards to viral replication [56-60]. Network analysis and comparison with known biological functions was used to add insights into potential mechanism of candidate hits.

Results

Viral Replication and Infectious Particles

Follow-up candidates were selected based upon z-scores and potential to participate in the viral life cycle. siRNA oligos were tested for their ability to modulate viral protein accumulation and viral replication. This was done at a single-cell resolution using immunofluorescence to detect viral proteins and to measure production of infectious particles. The majority of siRNA pools that deflect cell death in response to infection resulted in reduced viral protein accumulation and reduced production of

infectious particles (Figure 3.1). Among this group were IVNS1ABP and the splicing factor SFPQ. These proteins directly interact with the viral pathogenicity factor NS1 and the viral polymerase [55] (Beatriz Fontoura, personal communication). This would suggest these proteins have a positive role in supporting the viral corruption of host machinery for viral protein production. This class also includes RRAGD, a small G-protein that supports the amino-acid responsiveness of mTOR as a component of the “ragulator” complex [61]. Several reports have highlighted the importance of viral induction of mTOR for viral replication, but the mechanism is unknown [58,62]. Given the participation of endosomes as a viral entry mechanism [63], it is tempting to speculate that RRAGD is a limiting host factor for viral corruption of mTOR regulation. Additional factors in this group are involved with the host defense response, p53-mediated death and vesicle maturation and trafficking.

IFITM3

Among the most potent members of the sensitizer class were the previously described proviral host factors IFITM3 and its homolog IFITM1. IFITM3 has been reported to be required for restriction of viral infection and is thought to act at viral entry [56,64]. These gene products are interferon responsive, and depletion was associated with enhanced viral pathogenicity and enhanced viral protein production as compared to

controls (Figure 3.1). The role of IFITM3 in HBEC response was confirmed as even low viral titers result in significant infection and cell death compared to controls (Figure 3.2). Surprisingly, cells depleted of IFITM3 produced fewer infectious particles as determined by secondary infection of MDCK cells with cell culture supernatants (Figure 3.1, 3.2). For these assays, transfected HBEC30 cells were infected with an MOI of 5 and supernatants were collected 24 hours post-infection and used to infect MDCK cell cultures. It is important to note that there is enhanced frequency as well as enhanced amplitude of viral protein accumulation upon IFITM3 depletion. Reduced infectivity may therefore be a consequence of either limiting host factors or disruption of viral protein/host factor stoichiometry required for assembly of viable viral particles. Of interest, HBEC30 cells, when depleted of IFITM3, still show enhanced cell death upon exposure to virus lacking the viral pathogenicity factor NS1, a viral protein known to block many of the innate immunity responses [65-69] (Figure 3.3). However, deletion of NS1 results in complete failure of infectious particle production even upon IFITM3 depletion (Figure 3.3). This is consistent with reports that place IFITM3's antiviral activity at the level of viral entry.

Data Integration and Network Analysis

The selective follow-up separated the tested hits into functional classes. Hits were separated based upon their response with regards to cell viability and viral replication. To further fill out these functional classes, my screen data was integrated with data sets from four genome-wide siRNA screens that measured influenza A replication as the end-point assay [56-59]. Candidate hits, siRNAs with z-scores that had an absolute value greater than three, were queried for behavior in the other screens. siRNAs from the other screens that altered viral replication more than 1.5 times the standard deviation were considered hits and were used to separate siRNAs into the four classes described previously (Figure 3.4).

To increase functional understanding of candidate hits, modulators of influenza A pathogenicity were also compared with two genome-wide siRNA screens for modulators of cell cycle progression [70,71]. This comparison revealed a significant intersection between cell cycle genes and siRNAs that modulated cell death in response to viral infection (Figure 3.5). This intersection included CDC2 and CHEK1. Both of these genes had been identified as sensitizers that appear to deflect the host death response. However, CDC2 and CHEK1 depletion show quite distinct consequences on G1 versus G2 arrest, suggesting their contribution to H1N1 infection may be independent of cell cycle control. CHEK1 has not

been previously isolated in viral pathogenicity or viral replication screens and will be discussed further later on.

Data from the screen was also crossed with three siRNA screens for modulators of HIV infection [72-74] (Figure 3.6) as well as an interferon-stimulated gene (ISG) set [75]. Crossover with the HIV data set revealed 44 overlapping genes that likely represent genes involved with multiple virus families (Table 3.1). Twenty-one genes from ISG were modulators of the death response to influenza A infection (Table 3.2).

miRNA Screen

As a mechanism to potentially reveal combinatorial contributions of gene function to viral pathogenicity, the original screen was repeated using a library of 426 human microRNA mimics. These reagents have the advantage of inducing multigenic perturbations, though accurate assignment of target space is a significant challenge. This effort identified a small cohort of miRNA mimics that either enhanced or deflected H1N1 pathogenicity (Figure 3.7). Eleven of these were further examined for consequences on H1N1 viral protein production in HBEC30 cells, which identified both pathogenicity sensitizers and resistors that enhanced or repressed viral replication (Figure 3.8). Of note, a test for “hits” that also have activity against the recent pandemic strain Cal/04/09 identified two miRNA mimics that impair Cal/04/09 protein production in A549 cells, hsa-

miR-495 and hsa-miR-519a, (Figure 3.8). To infer biological processes that may be engaged by the miRNAs that can impair H1N1 replication, I examined the intersection of predicted miRNA targets and single-gene perturbations that behaved similarly to the subject miRNA. Candidate miRNA target genes were selected based on seed sequence presence in 3' UTRs as defined by Target Scan context scores. These predictions were intersected with siRNA data from this study and those of the 4 whole-genome siRNA screens that measured influenza virus replication [56-59]. When considered as a heuristic, this analysis produced three subnetworks that may correspond to the miRNA mode of action, namely the glycosylphosphatidylinositol transamidase, viral and host protein ubiquitylation [76,77] and alternative mRNA splicing (Figure 3.9).

Discussion

Here I have shown the ability to parse candidate hits from the original screen into four functional classes by the measurement of viral protein accumulation and infectious particle production. These classes I have termed: "infectious proviral host factors", "death effectors", "death deflecting proviral host factors", and "restriction factors". It should be noted that HBECs produce very little measurable infectious particles and, as a result, this can be hard to measure. The data presented here is

reproducible but shows a high variability. These functional classes can be used to predict the role a target has in viral life cycles. Genes that fall in the infectious proviral host factor class have therapeutic interest. The depletion of these genes results in increased cell viability and decreased viral protein production. The strongest resistor, CNTN2, falls into this class of genes. CNTN2 is a GPI anchored membrane protein, and is a good candidate for future studies therapeutic potential. Genes that fall into the death effectors category are interesting as they can give insight into the mechanism behind the death response. Two PI3K regulatory proteins fit into this category. PI3K signaling is known to be involved in the death response to influenza infection. A useful experiment would be to see if the overproduction of these regulatory proteins had the opposite effect on death in response to viral infection. The death deflecting proviral host factors also have therapeutic potential. These genes, when depleted, decrease cell viability but also decrease protein production. One of the most robust members of this family is COPB2, a COPII vesicle family. The final group, the restriction factors, represents the class of genes that are likely to be involved in innate immunity. Indeed, among the restriction factors I identified was IFITM3. At the time of identification, little was known about the IFITM proteins, but they have subsequently been shown to be innate immunity genes, which our data predicted and supports.

Interestingly, IFITM3 depletion resulted in decreased infectious particles. The mechanism behind this is unclear, but a possible explanation would be the increased viral proteins overload the system and fewer infectious particles are made.

To increase the functional classification and mechanistic understanding, I leveraged published data sets for integration with my data set. This resulted in the identification of a cell cycle influence on the outcome of infection. Interestingly, some of the cell cycle genes may affect phenotype in a cell cycle autonomous manner, as genes with differing cell cycle responses have similar effects on infection outcome. The comparison of influenza A hits with HIV hits identified genes that could play a broad role in fighting viral infections.

Finally, I was able to integrate siRNA-screening data with a miRNA screen. miRNAs target multiple genes that can be in the same pathway. The targeting of multiple genes can give rise to a stronger phenotype than a single gene approach. Comparing the siRNA data to the miRNA data can identify pathways that might have been overlooked with the siRNA data alone as a result of of weak phenotypes in the siRNA data. For example, the miRNA mimic 519a targets several members of the PIG family. The members of this family of proteins are weakly targeted in my screen and in several other influenza A screens. The strong phenotype

seen in the miRNA mimic experiments could be a result of targeting multiple PIG members at the same time, and may represent a potential therapeutic target.

Materials and Methods

Detection of Viral Protein

HBECs were reverse transfected and imaged for viral protein as described in Chapter II. Imaged cells were segmented and analyzed with Attovision software. Cells were recognized and segmented by Hoescht staining and distance from nucleus. Whole cell fluorescence intensity was measured and calculated with Attovision software.

Infectious Particles

HBECs were infected with WSN virus and supernatants were collected at 24 hours post-infection. Supernatants were then added to MDCK cells at 10%, 1%, and 0.1% final concentration, and MDCKs were fixed 14 hours after supernatant addition. Viral production in MDCK cells was detected as described above.

Functional Class Assignment

z-scores from four siRNA screens with viral replication were obtained from Christian Frost and compared to the 235 candidate hits identified in this study. z-scores with an absolute value greater than 1.5 were used to

classify hits. In cases where screens had opposite response, the higher z-score was used.

Data Set Comparisons

Published hits for cell cycle regulators, HIV regulators, and ISGs were obtained and overlapped with the z-scores from this study that had an absolute value of greater than 2.

miRNA Screen

The miRNA screen was performed with the Dharmacon miRNA mimic library targeting 426 miRNAs. The screen was performed identically to the siRNA screen, except for a 72-hour incubation between transfection and infection.

miRNA Predicted Networks

miRNA predicted targets were identified using target scan, and networks were built with the website Ingenuity.

H1/N1 Pandemic Virus

A549 cells were infected with the pandemic H1/N1 strain Cal/04/09 at an MOI of 1 and viral protein was detected by western blot as described in chapter 2. Mirco Schmolke performed all pandemic infections, and collected samples were given to me for viral protein detection.

Figures

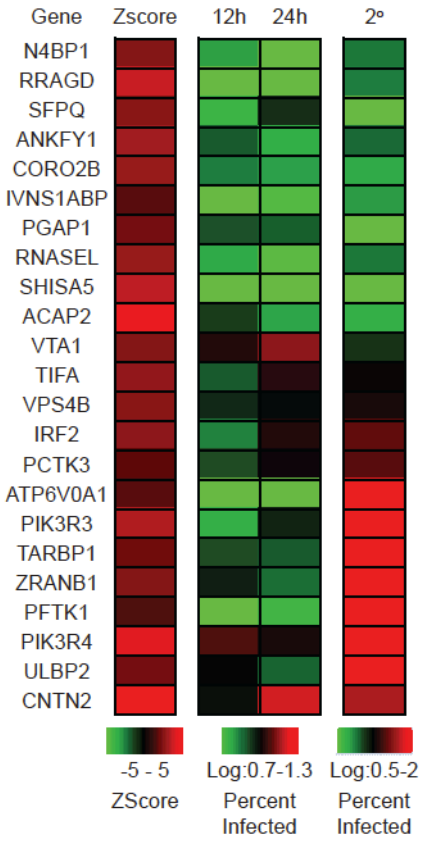
Gene
Zscore
12h
24h
2°
N4BP1
RRAGD
SFPQ
ANKFY1
CORO2B
IVNS1ABP
PGAP1
RNASEL
SHISA5
ACAP2
VTA1
TIFA
VPS4B
IRF2
PCTK3
ATP6V0A1
PIK3R3
TARBP1
ZRANB1
PFTK1
PIK3R4
ULBP2
CNTN2
-5 - 5
ZScore
Log:0.7-1.3
Percent
Infected
Log:0.5-2
Percent
Infected

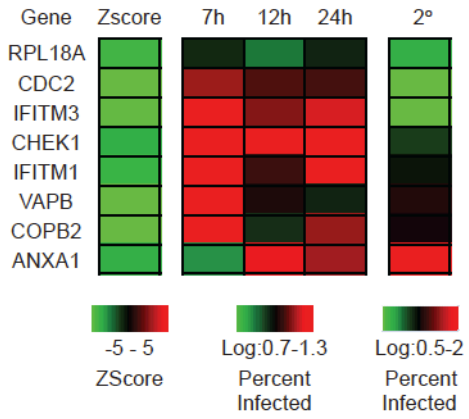
Gene
Zscore
7h
12h
24h
2°
RPL18A
CDC2
IFITM3
CHEK1
IFITM1
VAPB
COPB2
ANXA1
-5 - 5
ZScore
Log:0.7-1.3
Percent
Infected
Log:0.5-2
Percent
Infected

Figure 3.1. Viral Replication

A panel of 33 siRNAs was assayed for viral protein accumulation and infectious particle production. HBEC30s were transfected with siRNA and infected with WSN at an MOI of 5. For primary infection, cells were fixed at indicated time points and viral protein was detected by immunostaining. Supernatants from infected cells were collected at 24 hours post-infection and used for secondary infection of MDCK cells with viral protein detection by immunostaining. Resistors are shown in the left panel and sensitizers in the right.

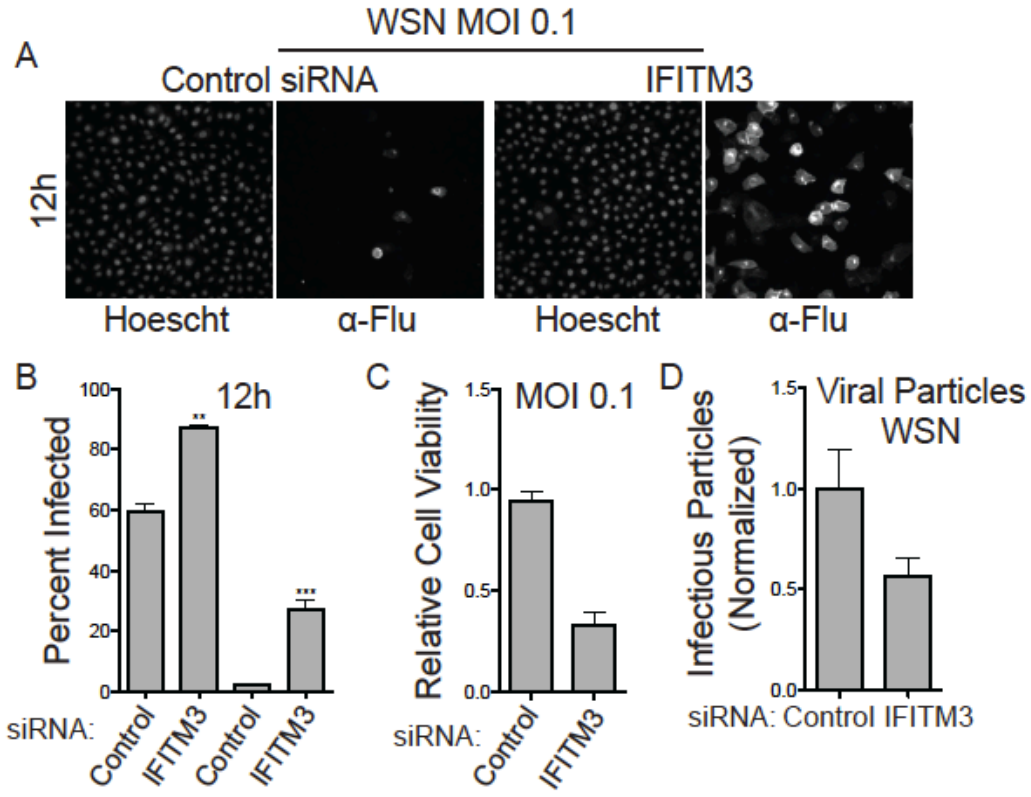

Figure 3.2. Role of IFITM3 in response to infection in HBEC-30

(A) HBECs were transfected with siRNA targeting IFITM3 or control siRNA and infected with WSN at an MOI of 0.1. Viral protein was detected at 12 hours post-infection by immunostaining with anti-influenza antibodies. (B) Cells treated in A were counted and the percent of infected cells was quantified. (C) Cells treated as in B were incubated 48 hours post-infection and cell viability was measured. (D) Supernatants from WSN infected HBEC30s were collected 24 hours post-infection and used for secondary infection of MDCK cells with viral protein detection by immunostaining. (P values; * < 0.05, ** < 0.01, *** < 0.0001)

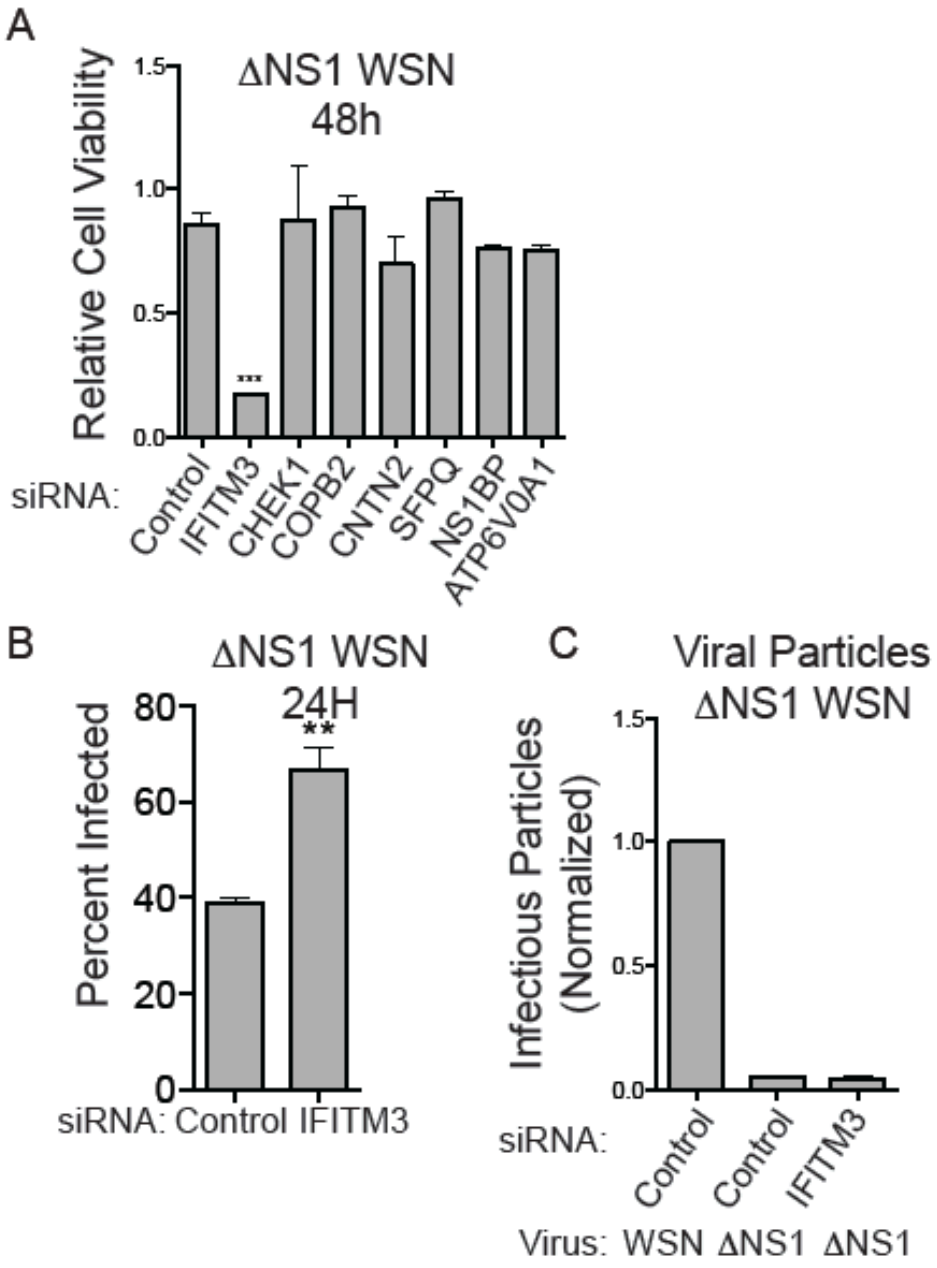

Figure 3.3 IFITM3 response to ΔNS1 Influenza A Virus

(A) HBEC30s were transfected with indicated siRNAs and infected with WSN lacking the viral protein NS1, cell viability was measured 48 hours post-infection. (B) Cells treated as in A were fixed at 24 hours post-infection and immunostained for viral protein for calculation of percentage of infected cells. (C) Supernatants from cells in A were used for secondary infection in MDCK cells and viral protein was detected by immunostaining. (P values; * < 0.05, ** < 0.01, *** < 0.0001)

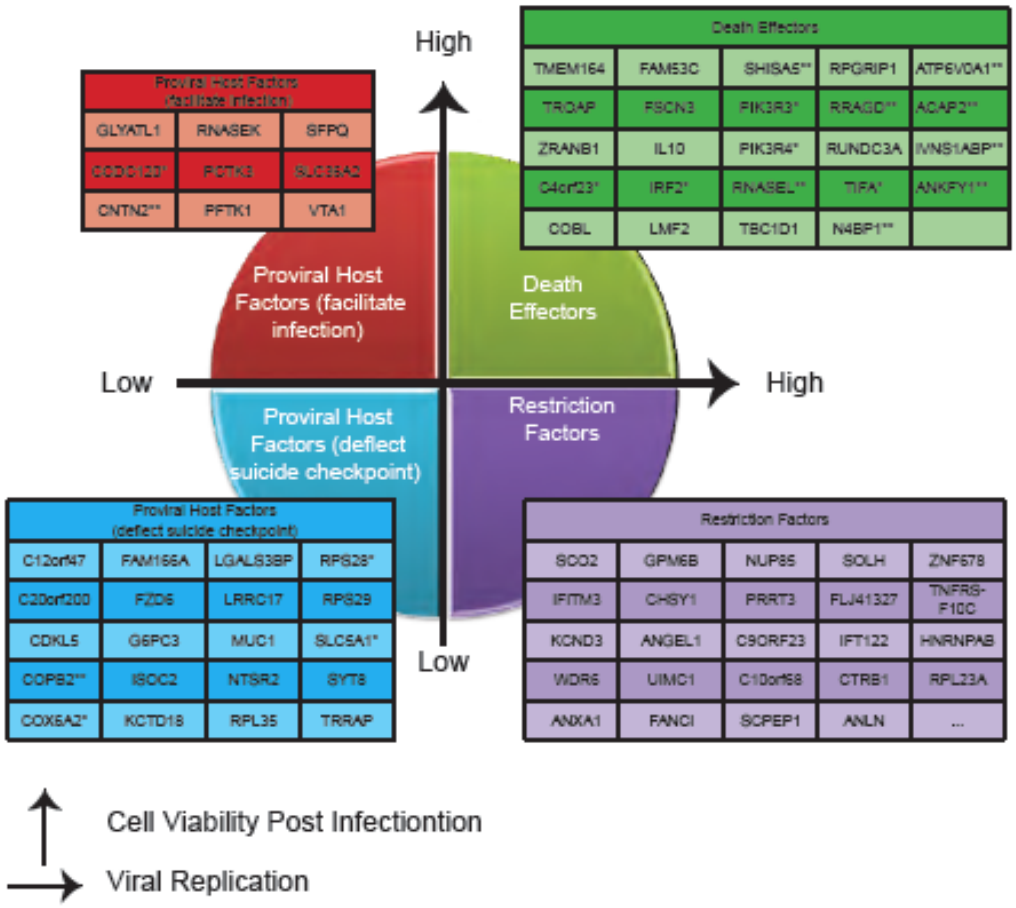

Figure 3.4 Functional Classes of influenza A Modulators

Cell viability data was queried against four published screens using viral replication as the end-point assay. Candidate hits were binned into functional classes based upon perturbation of viral cytopathogenicity together with viral replication.

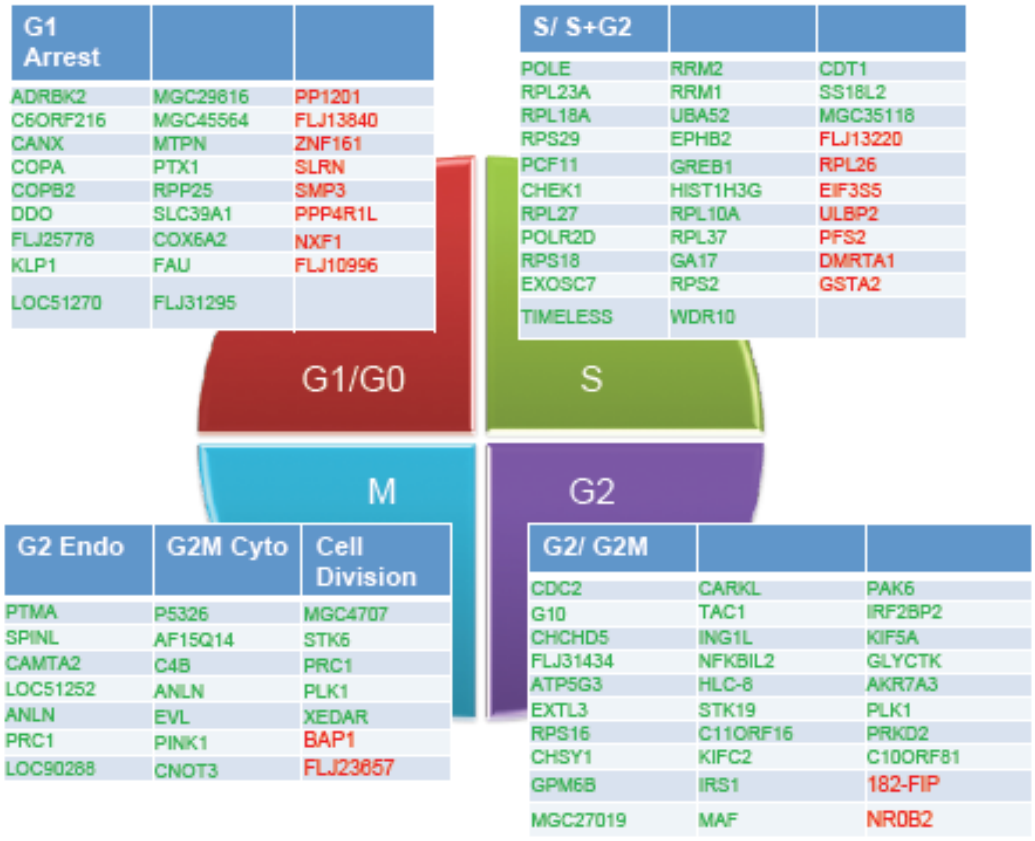

Figure 3.5. Cell Cycle Genes Involved in influenza A infection

siRNA screen results from this study were compared with data from two published screens for cell cycle modulators and the overlap is shown

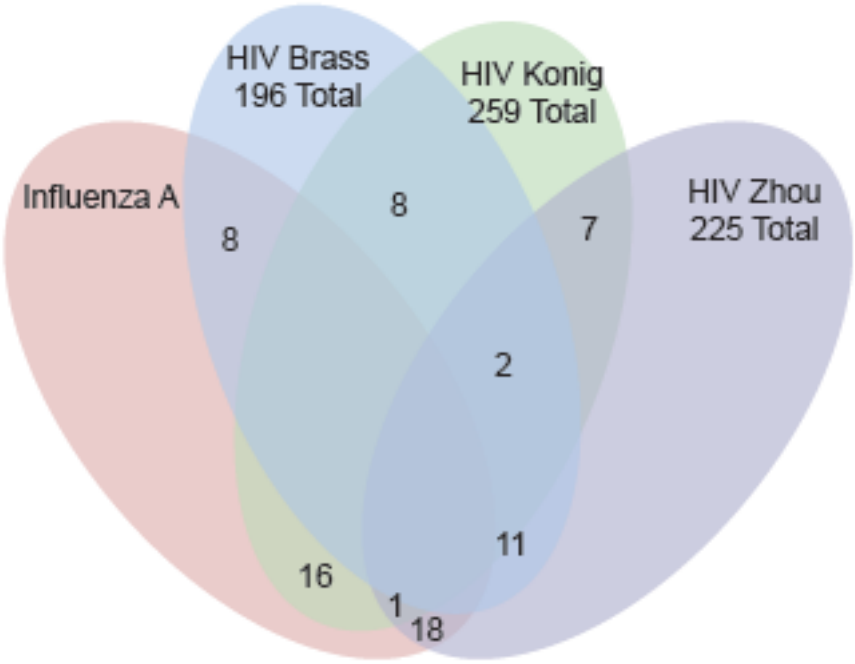

Figure 3.6 Overlap with regulators of HIV infection

Regulators of HIV identified in three published siRNA screens were crossed with the data set generated from this screen to identify global viral regulators with an overlap of 42 genes.

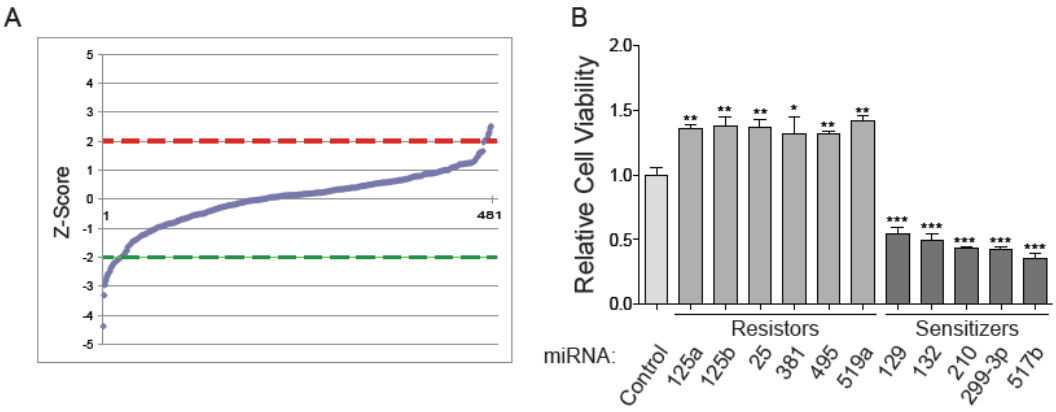

Figure 3.7 miRNA Modulators of the Death Response to Influenza A

(A) HBEC30s were transfected with miRNA mimics and screened using conditions identical to the siRNA screen. Z-scores were calculated for individual oligos and plotted according to rank order. Dashed lines indicate 2 standard deviations above (red) and below (green) the mean of the distribution. (B) HBEC30s were transfected with selected miRNA mimics, infected with WSN and cell viability phenotype was measured 48 hours post-infection. (P values; * < 0.05, ** < 0.01, *** < 0.0001)

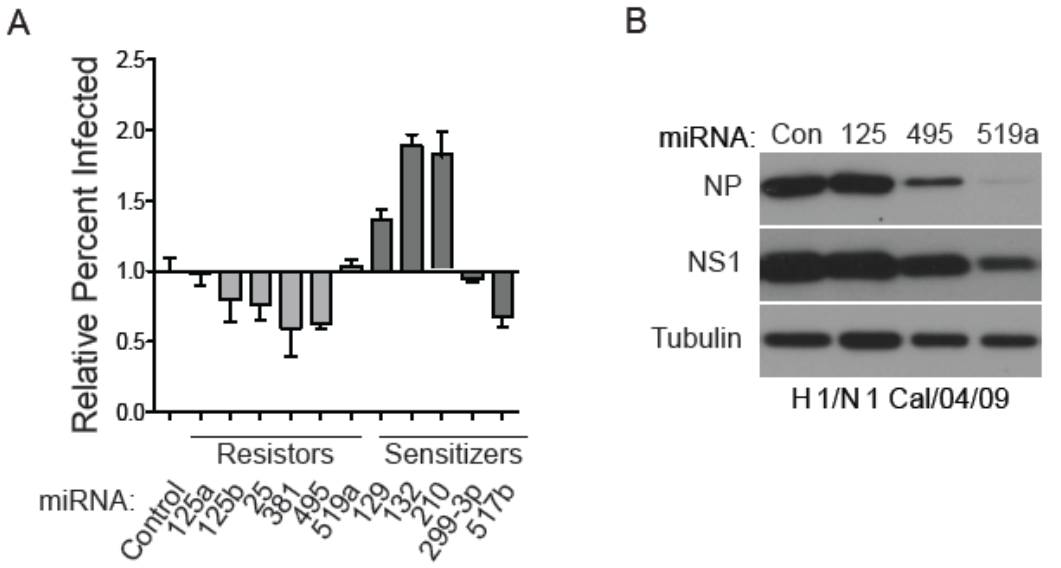

Figure 3.8 Inhibition of Viral Replication by miRNAs

(A) Cells treated as in figure 3.7 were fixed and immunostained for viral protein 12 hours post-infection. (B) A549 cells were transfected with miRNA mimics and infected with pandemic H1N1. Cell lysates were collected 24 hours post-infection and viral proteins were detected by immunoblotting.

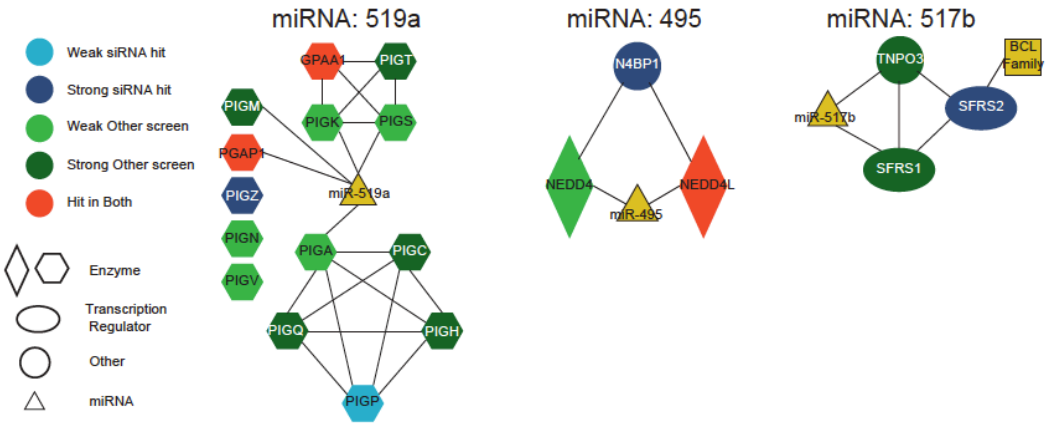

Figure 3.9. Identification of Key Pathways in Viral Life Cycle

Network analysis of predicted miRNA targets. Predicted targets were obtained from TargetScan and network analysis was performed with Ingenuity. Edges represent protein-protein interactions.

Table 3.1 Overlap with HIV screens				
ANKFY1	FAM178B	NXF1	RPL10A	STXBP1
ATP6V0A1	FLJ40125	PCSK6	S100A1	UBE2H
CCAR1	FLJ43860	PLK1	SERPINB6	VPS4A
CHST1	HIBCH	POLE	SF3B2	ZCCHC17
CLTA	IKBKG	PRKX	SFRS2	ZNF292
DDO	MAT2A	PSME2	SLC10A1	
DDX49	MRPL24	RAPGEF1	SLC2A13	
DUSP16	NR0B2	RBM25	SPG7	
EGFR	NUP62	RNASEL	SSR1	

Table 3.2 Overlap with ISG gene set			
IFITM3	GTPBP1	IRF9	AIM2
NAPA	PTMA	IL6ST	STEAP4
TMEM51	SLC25A30	PUS1	C9orf91
TAP2	USP18	STARD5	IRF2
UNC84B	PRKD2	ANKRD22	ANKFY1

CHAPTER IV: CHEMICAL VALIDATION OF THERAPEUTIC TARGETS

Introduction

Of the four categories identified in the follow-up studies, two were of great interest for their potential therapeutic value. As expected, several candidates were discovered that deflect cell death and inhibit viral production. Less intuitive, is the class of hits that enhance cell death but inhibit viral production. This group likely allows the cells to engage apoptosis upon infection without interference from the virus, which could provide a protective effect. In this chapter, I will show chemical validation that these pathways have real therapeutic potential.

Results

CHEK1 Inhibition

The initial screen and follow-up revealed CHEK1 as a potential deflector of the suicide response in influenza A infected cells. To investigate additional processes associated with CHEK1, I generated a context-specific protein-protein interaction sub-network. The context for this subnetwork was defined by the z-score distribution of the primary

screen (Figure 4.1). This sub-network revealed the circadian gene Timeless within the first-degree neighborhood of CHEK1 (Figure 4.2). Timeless is a gene that has recently been identified as a master regulator of the viral response [78]. These observations suggest CHEK1 has potential as a therapeutic target. To investigate this possibility, I used the chemical SB218078 to inhibit CHEK1 activity. SB218078 is an investigational CHEK1 inhibitor similar to one currently in clinical trials as an anti-neoplastic agent. It has an *in vitro* IC50 of 0.015μM and a $K_{i,app.}$ of 15±4 [79,80]. Pretreatment of cultures with 1 uM or 100 nM of SB218078 for 12 hours resulted in significant inhibition of viral protein accumulation. This was combined with a virus-specific death response 24 hours post-infection (Figure 4.3). At the 100 nM dose, viral protein was detectable; however, when viewed at a single cell resolution, viral protein production was severely limited (Figure 4.3). These observations suggest that SB218078 is releasing a death response that would otherwise be suppressed during the viral replication cycle. This virus-dependent death response is consistent with the experiments done using siRNA to deplete CHEK1. In cells depleted of CHEK1 via siRNA, there is an increase in the percentage of cells infected. However, the total number of cells is significantly reduced by 24 hours post-infection. Both pharmacological inhibition of CHEK1, and siRNA-mediated depletion show a virus-

dependent death response. The difference that is seen, between the two, in the percentage of infected cells is likely a consequence of incomplete depletion by siRNA resulting in residual cell populations with CHEK1 activity. Notably, SB218078 had no effect on H1N1 replication in A549 cells (Figure 4.5). A549 cells are a cancer cell line often used as a model for influenza A infection, including genomic-wide siRNA screens for modulators of viral pathogenicity. In contrast, a nontransformed, telomerase-immortalized mucosal epithelial cell line derived from a different patient, HBEC3 [81], was identical to HBEC30 in its responsiveness to SB218078 (Figure 4.6). These observations indicate intervention targets may be available in normal cells that are uncoupled from host regulatory networks in cancer cells, and this could explain why CHEK1 was not identified in other efforts to date that have universally relied on cancer lines as screen hosts.

RabGTTase Inhibition

One challenge to siRNA-screening efforts is the generation of false negatives. False negatives can arise when siRNA oligos do not efficiently deplete their target genes. One way to overcome this challenge is to employ coherent behavior of gene sets to identify key biological processes supporting a phenotype, rather than relying solely on an arbitrary scoring

threshold for each individual gene. I obtained a network analysis that had employed Netwalk [82] to facilitate identification of such gene sets based on overrepresentation of functionally coherent subnetworks within the graph. One such subnetwork implicated the prenylation of Rab-family GTPases in supporting replication of H1N1 (Figure 4.1). To test this observation, I employed 3-IPEHPC, a specific inhibitor of the type II Geranylgeranyl-transferases with an IC50 of 1.27μM and a K_i of 0.211μM for Rab1a modification [83]. As such, 3-IPEHPC specifically inhibits modification of Rab-family proteins with a carboxy-terminal CC motif, as opposed to the carboxy-terminal CAAX motif [83]. HBECs cells pretreated with 3-IPEHPC for 24 hours were significantly refractory to infection by H1N1 (Figure 4.6). Inhibitory activity was observed at concentrations as low as 125 nM (Figure 4.7). Unlike SB218078, A549 cells were also responsive to 3-IPEHPC (Figure 4.8). Importantly, 3-IPEHPC was protective against infection with the avian strain H5N1 and the recent pandemic swine flu strain H1N1 (Figure 4.8).

Discussion

The parsing of candidate hits into functional classes suggested two classes with particular therapeutic potential: death response proviral host

factors and infectious proviral host factors. One pathway from each group was selected for chemical validation of therapeutic potential.

HBECs treated with SB218078 showed an inhibition of viral protein accumulation. Interestingly, this was significantly stronger than the phenotype seen with the depletion of CHEK1 protein via siRNA. In fact, CHEK1 depletion actually showed an increase in the percentage of infected cells; however, this increase seems to be a result of increased cell death at early time points rather than an increase in the number of infected cells. This observation is consistent with chemical inhibition of CHEK1. Inhibition of CHEK1 with SB218078 results in an increased death response upon exposure to influenza A virus. The stronger phenotype of SB218078 can be explained by two possibilities. First, the siRNA depletion could be incomplete, resulting in a hypomorphic response; in comparison, the chemical inhibition might have a more complete inhibition of activity. Second, SB218078 also has some activity towards CDC2, a gene with the same phenotype of early cell death as CHEK1. The strength of the SB218078 phenotype could be a result of targeting both CDC2 and CHEK1 simultaneously. Interestingly, SB218078 had no effect on viral replication when tested in a cancer cell line, implying the possibility that A549s have mutations that overcome the cell checkpoint response to influenza A.

The second pathway targeted was the RabGGTase pathway which is involved in vesicle trafficking, a major part of the viral life cycle. Targeting a pathway, as opposed to a single gene, is valuable because it has the potential to overcome cell-specific and/or strain-specific requirements that single target may not. In the case of 3-IPEHPC, this is supported by the fact that the drug showed activity against three influenza A strains tested.

Materials and Methods

Network Analysis

Network analysis was obtained from Kakajan Komurov, who used his recently published method Netwalk [82].

Cell Culture

HBEC30-KT cells were cultured in KSFM with 1% pen/strep antibiotics. MDCK and A549 cells were grown in DMEM with 10% FBS.

Drugs

HBECs or A549 cells were plated on 96-well plates overnight. Media was removed and replaced with media containing SB218078 (1μM, 100nM 10nM) 3-IPEHPC (12.5μM, 1.25μM, 125nM) DMSO (0.06%) or plain media. Cells were incubated overnight and then infected with WSN at an MOI of 5. Cells were fixed with 4% formaldehyde at 8 hours, 12 hours and

24 hours post-infection and stained as described previously. SB218078 was purchased from Tocris biosciences cat # 2560 and dissolved in DMSO. 3-IPEHPC, a gift from Dr. McKenna at USC, was dissolved in PBS.

Viruses

A549 cells were infected with either the H5N1 strain influenza A/VietNam/1203/2004 or the pandemic H1N1 strain Cal/04/09 at an MOI of 1, and viral protein was detected by western blot as described in Chapter II. Mirco Schmolke performed all H5N1 and pandemic infections, and collected samples were given to me for viral protein detection.

Figures

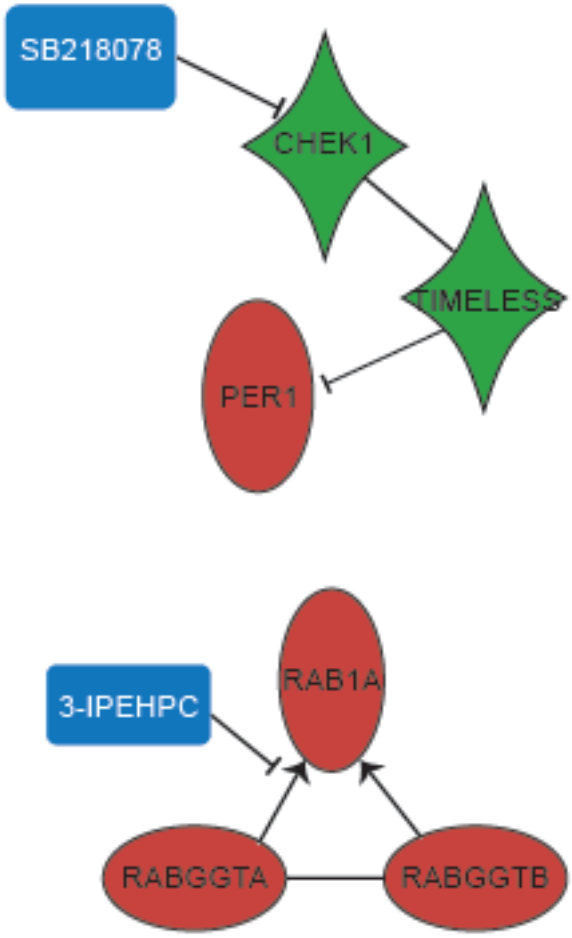

Figure 4.1. Pathways for Chemical Validation

Network analysis with Netwalk revealed two pharmacologically addressable pathways as shown.

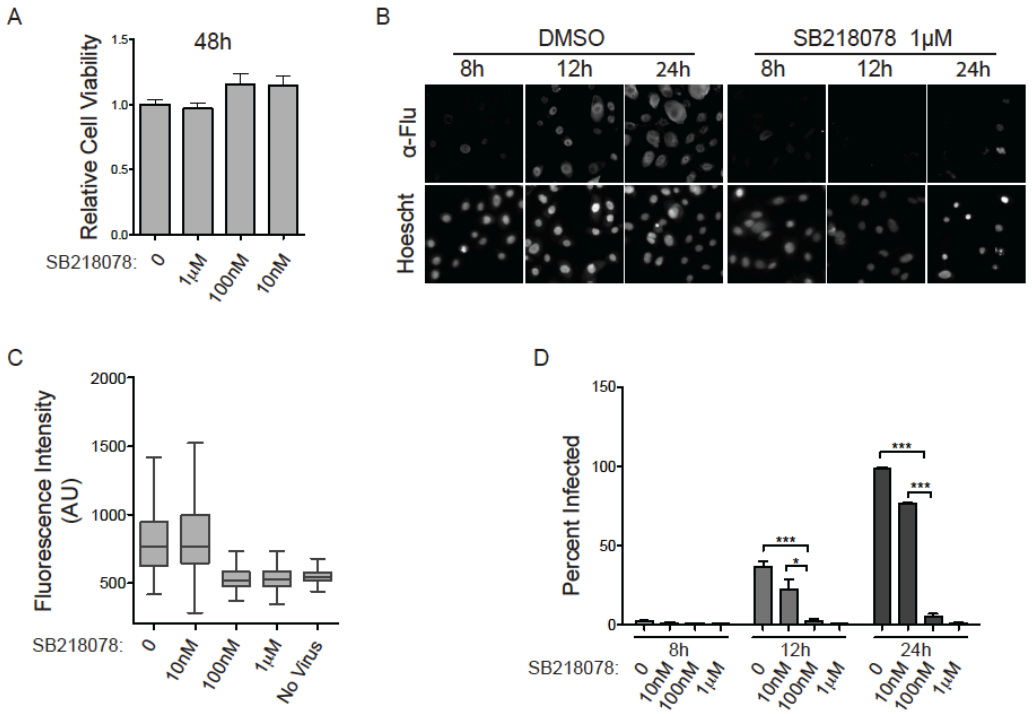

Figure 4.2 CHEK1 Mediated Viral Replication Inhibition

(A) HBEC30s were treated with SB218078 at indicated concentrations and cell viability was measured after 48 hours. (B) HBEC30s were treated as in A and infected with WSN at an MOI of 5 followed by immunostaining at indicated time points. Top panels show anti-influenza A staining and bottom panels, labeled Hoescht, show nuclear staining with Hoescht. (C) Fluorescence intensity was measured and quantified from B. (D) Percentage of infected cells from B. (P values; * < 0.05, ** < 0.01, *** < 0.0001)

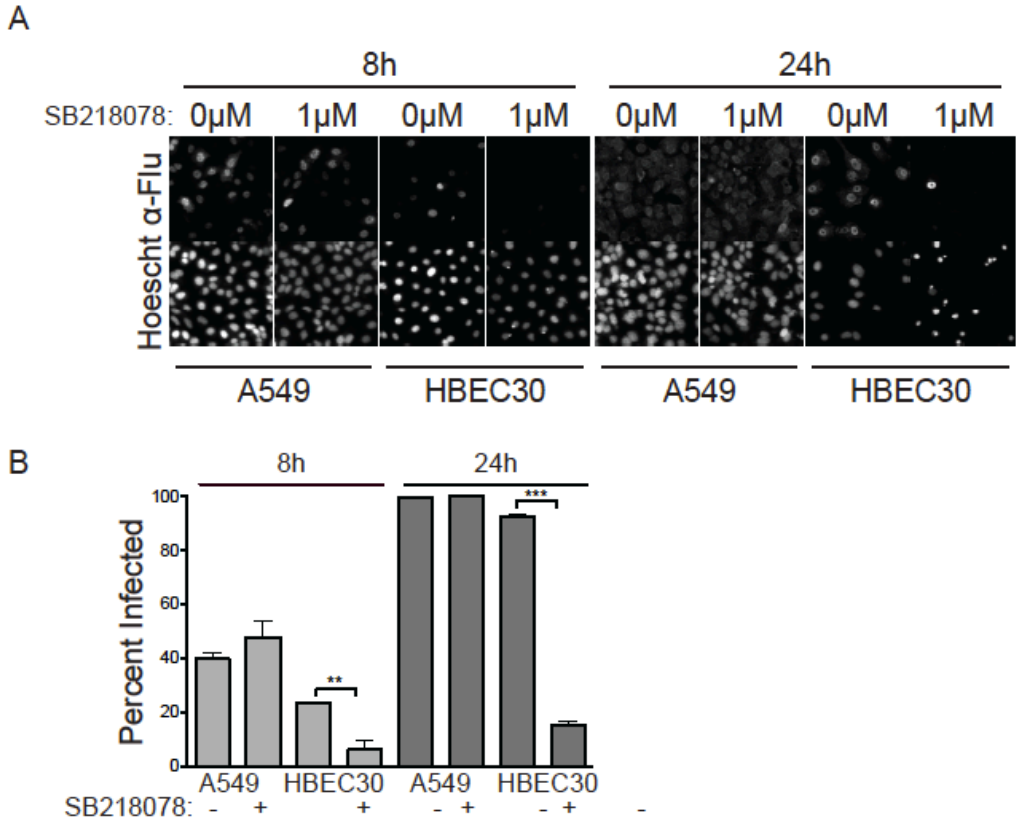

Figure 4.3 A549 Cells Fail to Respond to CHEK1 Inhibition

(A) A549 cells were pretreated with 218078 and infected with WSN at an MOI of 5. Viral protein was detected by immunostaining. Top panels show anti-influenza A staining and bottom panels, labeled Hoescht, show nuclear staining with Hoescht. (B) Quantification of percent of infected cells in E. (P values; * < 0.05, ** < 0.01, *** < 0.0001)

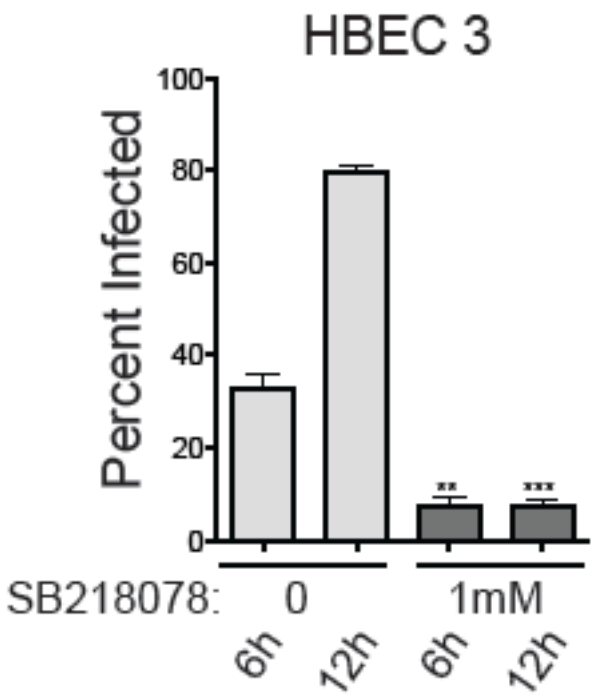

Figure 4.4 CHEK1 Mediated Viral Inhibition in HBEC-3 cells

HBEC3-KT cells were pretreated with 218078, infected with WSN at an MOI of 5 and immunostained for detection of viral protein. The percentage of infected cells was quantified. (P values; * < 0.05, ** < 0.01, *** < 0.0001)

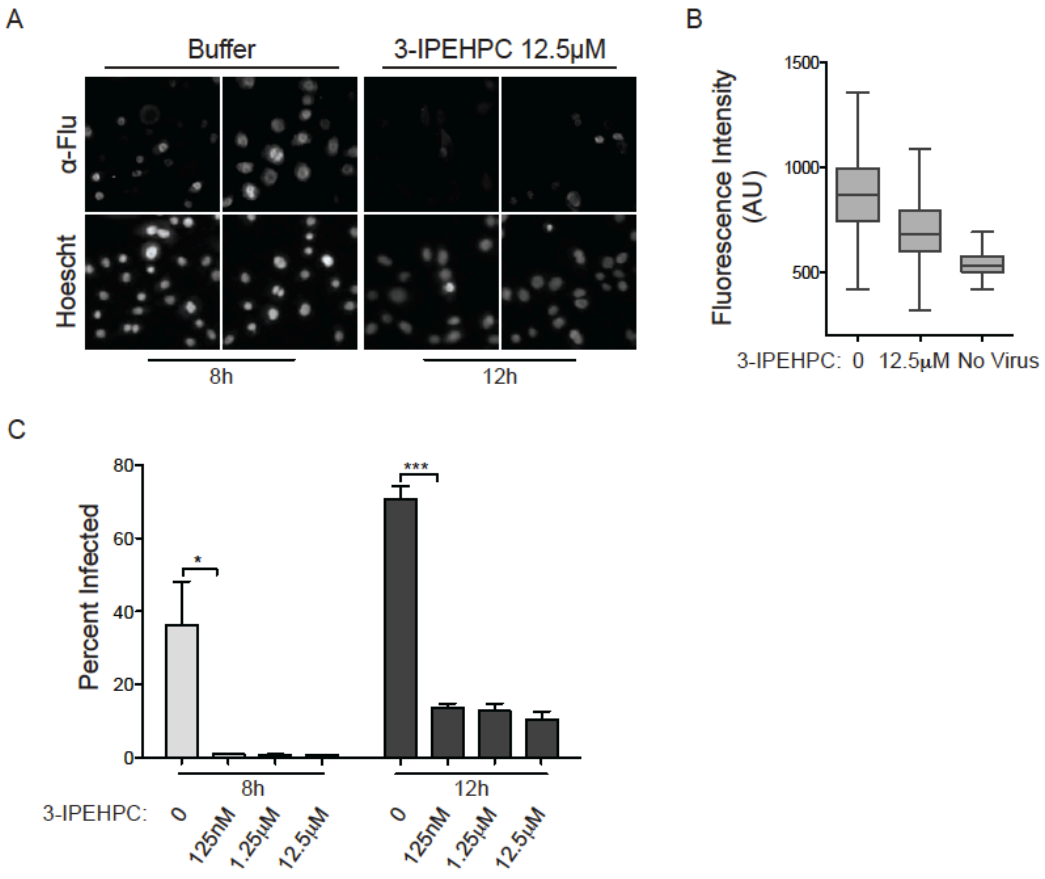

Figure 4.5 3-IPEHPC Inhibition of Viral Replication

(A) HBEC30s were pretreated with 3-IPEHPC or buffer and infected with WSN at an MOI of 5. Viral protein was detected by immunostaining. Top panels show anti-influenza A staining and bottom panels, labeled Hoescht, show nuclear staining with Hoescht. (B) Overall fluorescence intensity of cells in A was quantified. (C) Quantification of percent of infected cells in A. . (P values; * < 0.05, ** < 0.01, *** < 0.0001)

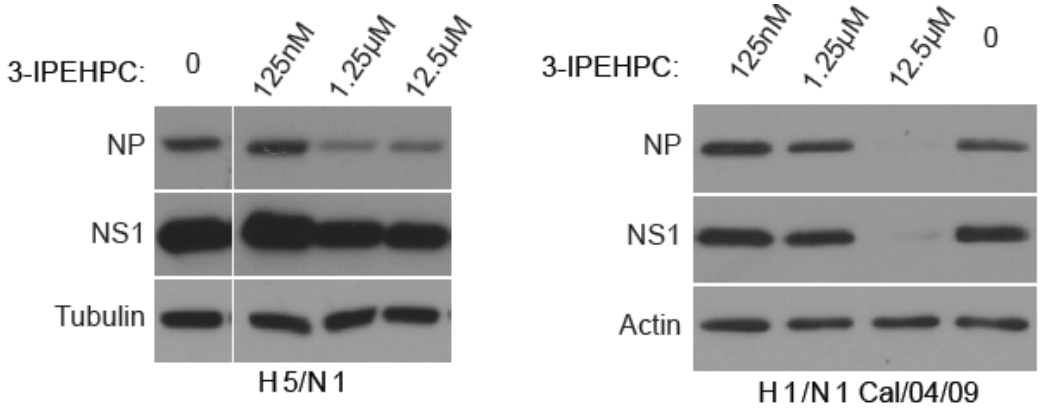

Figure 4.6 3-IPEHPC Inhibition of Multiple Influenza A Strains

A549 cells were pretreated with 3-IPEHPC and infected with either avian H5N1 or the recent H1N1 pandemic strain. Lysates from infected cells were collected 24 hours post-infection and viral protein was detected by immunoblot

CHAPTER V: DISCUSSION AND FUTURE DIRECTIONS

In this work, I have focused on the identification of human genes that modulate the death response to influenza A virus infection. This was done in human bronchial airway epithelial cells to maximize physiologically relevance. This cell type was selected as a tissue culture model that maintains cell autonomous biological features representative of the viral target tissue. Of interest, HBECs resist plaque formation, but they are highly sensitive to single cycle infection. The resistance to plaque formation may be a result of the immune response in HBECs. Genome-wide siRNA screening identified resistors and sensitizers to virus-dependent cell death. One of the major points identified in this analysis was the identification of gene products that serve to restrain the cell death response that would otherwise be engaged upon detection of viral infection. These genes are not required to support normal cell viability; however, in the presence of virus, depletion of these genes enhanced the death response and decreased viral protein accumulation. As such, this class may represent targets for interventions that restrain propagation of multi-cycle infection by facilitating suicide of infected cells prior to production of new infectious particles. A chemically addressable member of this class, CHEK1, showed strong activity in multiple HBEC lines but

not in A549 cells, a non-small cell lung tumor-derived line commonly employed to model influenza virus infection. This observation suggests that intervention targets may be available in normal epithelial cells that are uncoupled from host regulatory networks in cancer cells. The ability to induce rapid apoptosis in response to viral infection has great therapeutic potential. Apoptosis is engaged as an anti-viral defense mechanism against other RNA viruses. Evidence suggests that this is also the case in ducks infected with avian influenza A. Influenza A is able to infect ducks but causes little to no pathological response. This is seen with strains that cause a rapid induction of apoptosis in cell culture. Interestingly, strains that cause pathological symptoms in ducks correlate with decreased onset of apoptosis. This suggests that the induction of apoptosis is a natural anti-viral strategy in aquatic fowl. Therefore, an approach that mimicked this natural defense could provide a powerful mechanism of treatment. Current viral drugs are increasingly becoming obsolete as viruses evolve to evade drug action. This will likely be true for newer classes of drugs that target host proteins as well, as the virus evolves to take advantage of redundancy in the targeted pathways. However, the lessons from aquatic fowls would suggest that the death modulators are one class of proteins that can be targeted without fear of becoming obsolete and would be a powerful tool in the expanding kit of influenza A treatment.

This work provides a springboard for multiple lines of future research. From it can be extracted information about the pathways involved in cell death as well as genes involved in innate immunity. Indeed, IFITM3 was identified in this screen prior to its publication as an innate immune gene. IFITM3 falls in the large class of genes that, when depleted, increase viral proteins and sensitivity to death upon exposure to influenza A. Further testing of this group would yield new innate immunity genes. It would be interesting to see how depletion of these genes effects plaque formation in HBEC cells in response to influenza A infection.

However, the focus of this work was to identify novel pathways for therapeutic treatment of influenza A virus. To further this, future work should be focused on moving potential hits into actual therapy in animal models. I identified two pathways that are amenable to chemical inhibition and show effectiveness in cell culture. One of these, CHEK1 inhibition, has potential as a cancer agent and several drugs targeting CHEK1 are under investigation for cancer therapy. This could lead to a quick turnaround for influenza A treatment, and further studies in animals should be performed. I also showed that 3-IPEHPC has therapeutic potential; however, it would need to be adapted to animal treatment and then tested in animal models. 3-IPEHPC is an exciting candidate because it targets a pathway and not a single gene. This increases it potential to act on

multiple viral strains and in multiple cell lines. Indeed, 3-IPEHPC effectively inhibited three viral strains and worked in three cell lines.

CHEK1 is only one of many examples of potential therapeutic targets in the class of modulators that enhance cell death upon exposure to virus. An understanding of the type of cell death caused by these modulators is important. One of the major contributors to the pathology of influenza is a cytokine storm, the quelling of which is under investigation as a therapeutic for influenza A infection [84,85]. It is possible that targets could limit viral production but at the expense of increasing the pathology. It would therefore be useful to have targets that increase the amount of apoptosis, which results in a less active inflammatory response compared with other forms of cell death. Measuring the response of candidate hits in regards to activation of CASPASE 3 and 7 will narrow the genes of interest. Candidates that show a large amount of increase in CASPASE activation would then be moved on for further studies in animal models. Where possible, this should be done in ferrets, which model both the pathogenicity and transmissibility of influenza A, as opposed to mice, which only show the pathogenicity and require mice-adapted influenza A. The further characterization and study of this class of hits may lead to future therapeutic treatment for influenza A virus.

BIBLIOGRAPHY

1. Knipe DM, Howley PM (2001) Fields Virology. Fourth Ed. Vol. 1. pp. : 1487-1531.
2. Micillo E, Bianco A, D'Auria D, Mazzarella G, Abbate GF (2000) Respiratory infections and asthma. Allergy 55 Suppl 61: 42-45.
3. Bright RA, Medina MJ, Xu X, Perez-Oronoz G, Wallis TR, et al. (2005) Incidence of adamantane resistance among influenza A (H3N2) viruses isolated worldwide from 1994 to 2005: a cause for concern. Lancet 366: 1175-1181.
4. Ludwig S, Planz O, Pleschka S, Wolff T (2003) Influenza-virus-induced signaling cascades: targets for antiviral therapy? Trends Mol Med 9: 46-52.
5. Helenius A (1992) Unpacking the incoming influenza virus. Cell 69: 577-578.
6. Matlin KS, Reggio H, Helenius A, Simons K (1981) Infectious entry pathway of influenza virus in a canine kidney cell line. J Cell Biol 91: 601-613.
7. Sieczkarski SB, Whittaker GR (2002) Influenza virus can enter and infect cells in the absence of clathrin-mediated endocytosis. J Virol 76: 10455-10464.
8. Rust MJ, Lakadamyali M, Zhang F, Zhuang X (2004) Assembly of endocytic machinery around individual influenza viruses during viral entry. Nat Struct Mol Biol 11: 567-573.
9. Mikulasova A, Vareckova E, Fodor E (2000) Transcription and replication of the influenza a virus genome. Acta Virol 44: 273-282.
10. Ludwig S, Pleschka S, Planz O, Wolff T (2006) Ringing the alarm bells: signalling and apoptosis in influenza virus infected cells. Cell Microbiol 8: 375-386.
11. Fensterl V, Sen GC (2009) Interferons and viral infections. Biofactors 35: 14-20.
12. Takaoka A, Hayakawa S, Yanai H, Stoiber D, Negishi H, et al. (2003) Integration of interferon-alpha/beta signalling to p53 responses in tumour suppression and antiviral defence. Nature 424: 516-523.
13. Samuel CE (2001) Antiviral actions of interferons. Clin Microbiol Rev 14: 778-809, table of contents.
14. Kujime K, Hashimoto S, Gon Y, Shimizu K, Horie T (2000) p38 mitogen-activated protein kinase and c-jun-NH2-terminal kinase regulate

RANTES production by influenza virus-infected human bronchial epithelial cells. J Immunol 164: 3222-3228.
15. Ludwig S, Ehrhardt C, Neumeier ER, Kracht M, Rapp UR, et al. (2001) Influenza virus-induced AP-1-dependent gene expression requires activation of the JNK signaling pathway. J Biol Chem 276: 10990-10998.
16. Pleschka S, Wolff T, Ehrhardt C, Hobom G, Planz O, et al. (2001) Influenza virus propagation is impaired by inhibition of the Raf/MEK/ERK signalling cascade. Nat Cell Biol 3: 301-305.
17. Ludwig S, Wolff T, Ehrhardt C, Wurzer WJ, Reinhardt J, et al. (2004) MEK inhibition impairs influenza B virus propagation without emergence of resistant variants. FEBS Lett 561: 37-43.
18. Pahl HL (1999) Activators and target genes of Rel/NF-kappaB transcription factors. Oncogene 18: 6853-6866.
19. Chu WM, Ostertag D, Li ZW, Chang L, Chen Y, et al. (1999) JNK2 and IKKbeta are required for activating the innate response to viral infection. Immunity 11: 721-731.
20. Bourteele S, Oesterle K, Pleschka S, Unterstab G, Ehrhardt C, et al. (2005) Constitutive activation of the transcription factor NF-kappaB results in impaired borna disease virus replication. J Virol 79: 6043-6051.
21. Nimmerjahn F, Dudziak D, Dirmeier U, Hobom G, Riedel A, et al. (2004) Active NF-kappaB signalling is a prerequisite for influenza virus infection. J Gen Virol 85: 2347-2356.
22. Wurzer WJ, Ehrhardt C, Pleschka S, Berberich-Siebelt F, Wolff T, et al. (2004) NF-kappaB-dependent induction of tumor necrosis factor-related apoptosis-inducing ligand (TRAIL) and Fas/FasL is crucial for efficient influenza virus propagation. J Biol Chem 279: 30931-30937.
23. Donelan NR, Dauber B, Wang X, Basler CF, Wolff T, et al. (2004) The N- and C-terminal domains of the NS1 protein of influenza B virus can independently inhibit IRF-3 and beta interferon promoter activation. J Virol 78: 11574-11582.
24. Lu Y, Qian XY, Krug RM (1994) The influenza virus NS1 protein: a novel inhibitor of pre-mRNA splicing. Genes Dev 8: 1817-1828.
25. Li Y, Yamakita Y, Krug RM (1998) Regulation of a nuclear export signal by an adjacent inhibitory sequence: the effector domain of the influenza virus NS1 protein. Proc Natl Acad Sci U S A 95: 4864-4869.
26. Guo Z, Chen LM, Zeng H, Gomez JA, Plowden J, et al. (2007) NS1 protein of influenza A virus inhibits the function of intracytoplasmic pathogen sensor, RIG-I. Am J Respir Cell Mol Biol 36: 263-269.

27. Zhirnov OP, Konakova TE, Wolff T, Klenk HD (2002) NS1 protein of influenza A virus down-regulates apoptosis. J Virol 76: 1617-1625.
28. Ehrhardt C, Wolff T, Pleschka S, Planz O, Beermann W, et al. (2007) Influenza A virus NS1 protein activates the PI3K/Akt pathway to mediate antiapoptotic signaling responses. J Virol 81: 3058-3067.
29. Fischer U, Schulze-Osthoff K (2005) Apoptosis-based therapies and drug targets. Cell Death Differ 12 Suppl 1: 942-961.
30. Mori I, Goshima F, Imai Y, Kohsaka S, Sugiyama T, et al. (2002) Olfactory receptor neurons prevent dissemination of neurovirulent influenza A virus into the brain by undergoing virus-induced apoptosis. J Gen Virol 83: 2109-2116.
31. Takizawa T, Matsukawa S, Higuchi Y, Nakamura S, Nakanishi Y, et al. (1993) Induction of programmed cell death (apoptosis) by influenza virus infection in tissue culture cells. J Gen Virol 74 (Pt 11): 2347-2355.
32. Fesq H, Bacher M, Nain M, Gemsa D (1994) Programmed cell death (apoptosis) in human monocytes infected by influenza A virus. Immunobiology 190: 175-182.
33. Mori I, Komatsu T, Takeuchi K, Nakakuki K, Sudo M, et al. (1995) In vivo induction of apoptosis by influenza virus. J Gen Virol 76 (Pt 11): 2869-2873.
34. Zhirnov OP, Konakova TE, Garten W, Klenk H (1999) Caspase-dependent N-terminal cleavage of influenza virus nucleocapsid protein in infected cells. J Virol 73: 10158-10163.
35. Wurzer WJ, Planz O, Ehrhardt C, Giner M, Silberzahn T, et al. (2003) Caspase 3 activation is essential for efficient influenza virus propagation. EMBO J 22: 2717-2728.
36. Hinshaw VS, Olsen CW, Dybdahl-Sissoko N, Evans D (1994) Apoptosis: a mechanism of cell killing by influenza A and B viruses. J Virol 68: 3667-3673.
37. Olsen CW, Kehren JC, Dybdahl-Sissoko NR, Hinshaw VS (1996) bcl-2 alters influenza virus yield, spread, and hemagglutinin glycosylation. J Virol 70: 663-666.
38. McLean JE, Datan E, Matassov D, Zakeri ZF (2009) Lack of Bax prevents influenza A virus-induced apoptosis and causes diminished viral replication. J Virol 83: 8233-8246.
39. Ishikawa E, Nakazawa M, Yoshinari M, Minami M (2005) Role of tumor necrosis factor-related apoptosis-inducing ligand in immune response to influenza virus infection in mice. J Virol 79: 7658-7663.

40. Brydon EW, Morris SJ, Sweet C (2005) Role of apoptosis and cytokines in influenza virus morbidity. FEMS Microbiol Rev 29: 837-850.
41. Kuchipudi SV, Dunham SP, Nelli R, White GA, Coward VJ, et al. (2011) Rapid death of duck cells infected with influenza: a potential mechanism for host resistance to H5N1. Immunol Cell Biol.
42. Whitehurst AW, Bodemann BO, Cardenas J, Ferguson D, Girard L, et al. (2007) Synthetic lethal screen identification of chemosensitizer loci in cancer cells. Nature 446: 815-819.
43. Kawasaki H, Taira K, Morris KV (2005) siRNA induced transcriptional gene silencing in mammalian cells. Cell Cycle 4: 442-448.
44. Zamore PD, Tuschl T, Sharp PA, Bartel DP (2000) RNAi: double-stranded RNA directs the ATP-dependent cleavage of mRNA at 21 to 23 nucleotide intervals. Cell 101: 25-33.
45. Elbashir SM, Lendeckel W, Tuschl T (2001) RNA interference is mediated by 21- and 22-nucleotide RNAs. Genes Dev 15: 188-200.
46. Liu J, Carmell MA, Rivas FV, Marsden CG, Thomson JM, et al. (2004) Argonaute2 is the catalytic engine of mammalian RNAi. Science 305: 1437-1441.
47. Tuschl T, Zamore PD, Lehmann R, Bartel DP, Sharp PA (1999) Targeted mRNA degradation by double-stranded RNA in vitro. Genes Dev 13: 3191-3197.
48. Czauderna F, Fechtner M, Dames S, Aygun H, Klippel A, et al. (2003) Structural variations and stabilising modifications of synthetic siRNAs in mammalian cells. Nucleic Acids Res 31: 2705-2716.
49. Castanotto D, Rossi JJ (2009) The promises and pitfalls of RNA-interference-based therapeutics. Nature 457: 426-433.
50. Bender A, Albert M, Reddy A, Feldman M, Sauter B, et al. (1998) The distinctive features of influenza virus infection of dendritic cells. Immunobiology 198: 552-567.
51. Vaughan MB, Ramirez RD, Wright WE, Minna JD, Shay JW (2006) A three-dimensional model of differentiation of immortalized human bronchial epithelial cells. Differentiation 74: 141-148.
52. Lu X, Masic A, Li Y, Shin Y, Liu Q, et al. (2010) The PI3K/Akt pathway inhibits influenza A virus-induced Bax-mediated apoptosis by negatively regulating the JNK pathway via ASK1. J Gen Virol 91: 1439-1449.
53. Fujioka Y, Tsuda M, Hattori T, Sasaki J, Sasaki T, et al. (2011) The Ras-PI3K signaling pathway is involved in clathrin-independent endocytosis and the internalization of influenza viruses. PLoS One 6: e16324.

54. Guinea R, Carrasco L (1995) Requirement for vacuolar proton-ATPase activity during entry of influenza virus into cells. J Virol 69: 2306-2312.
55. Bortz E, Westera L, Maamary J, Steel J, Albrecht RA, et al. (2011) Host- and strain-specific regulation of influenza virus polymerase activity by interacting cellular proteins. MBio 2.
56. Brass AL, Huang IC, Benita Y, John SP, Krishnan MN, et al. (2009) The IFITM proteins mediate cellular resistance to influenza A H1N1 virus, West Nile virus, and dengue virus. Cell 139: 1243-1254.
57. Karlas A, Machuy N, Shin Y, Pleissner KP, Artarini A, et al. (2010) Genome-wide RNAi screen identifies human host factors crucial for influenza virus replication. Nature 463: 818-822.
58. Konig R, Stertz S, Zhou Y, Inoue A, Hoffmann HH, et al. (2010) Human host factors required for influenza virus replication. Nature 463: 813-817.
59. Shapira SD, Gat-Viks I, Shum BO, Dricot A, de Grace MM, et al. (2009) A physical and regulatory map of host-influenza interactions reveals pathways in H1N1 infection. Cell 139: 1255-1267.
60. Watanabe T, Watanabe S, Kawaoka Y (2010) Cellular networks involved in the influenza virus life cycle. Cell host & microbe 7: 427-439.
61. Sancak Y, Bar-Peled L, Zoncu R, Markhard AL, Nada S, et al. (2010) Ragulator-Rag complex targets mTORC1 to the lysosomal surface and is necessary for its activation by amino acids. Cell 141: 290-303.
62. Mata MA, Satterly N, Versteeg GA, Frantz D, Wei S, et al. (2011) Chemical inhibition of RNA viruses reveals REDD1 as a host defense factor. Nat Chem Biol 7: 712-719.
63. Skehel JJ, Wiley DC (2000) Receptor binding and membrane fusion in virus entry: the influenza hemagglutinin. Annu Rev Biochem 69: 531-569.
64. Huang IC, Bailey CC, Weyer JL, Radoshitzky SR, Becker MM, et al. (2011) Distinct patterns of IFITM-mediated restriction of filoviruses, SARS coronavirus, and influenza A virus. PLoS Pathog 7: e1001258.
65. Tisoncik JR, Billharz R, Burmakina S, Belisle SE, Proll SC, et al. (2011) The NS1 protein of influenza A virus suppresses interferon-regulated activation of antigen-presentation and immune-proteasome pathways. J Gen Virol 92: 2093-2104.
66. Meunier I, von Messling V (2011) NS1-mediated delay of type I interferon induction contributes to influenza A virulence in ferrets. J Gen Virol 92: 1635-1644.

67. Jia D, Rahbar R, Chan RW, Lee SM, Chan MC, et al. (2010) Influenza virus non-structural protein 1 (NS1) disrupts interferon signaling. PLoS One 5: e13927.
68. Wang X, Shen Y, Qiu Y, Shi Z, Shao D, et al. (2010) The non-structural (NS1) protein of influenza A virus associates with p53 and inhibits p53-mediated transcriptional activity and apoptosis. Biochem Biophys Res Commun 395: 141-145.
69. Haye K, Burmakina S, Moran T, Garcia-Sastre A, Fernandez-Sesma A (2009) The NS1 protein of a human influenza virus inhibits type I interferon production and the induction of antiviral responses in primary human dendritic and respiratory epithelial cells. J Virol 83: 6849-6862.
70. Mukherji M, Bell R, Supekova L, Wang Y, Orth AP, et al. (2006) Genome-wide functional analysis of human cell-cycle regulators. Proc Natl Acad Sci U S A 103: 14819-14824.
71. Kittler R, Pelletier L, Heninger AK, Slabicki M, Theis M, et al. (2007) Genome-scale RNAi profiling of cell division in human tissue culture cells. Nat Cell Biol 9: 1401-1412.
72. Konig R, Zhou Y, Elleder D, Diamond TL, Bonamy GM, et al. (2008) Global analysis of host-pathogen interactions that regulate early-stage HIV-1 replication. Cell 135: 49-60.
73. Zhou H, Xu M, Huang Q, Gates AT, Zhang XD, et al. (2008) Genome-scale RNAi screen for host factors required for HIV replication. Cell Host Microbe 4: 495-504.
74. Brass AL, Dykxhoorn DM, Benita Y, Yan N, Engelman A, et al. (2008) Identification of host proteins required for HIV infection through a functional genomic screen. Science 319: 921-926.
75. Schoggins JW, Wilson SJ, Panis M, Murphy MY, Jones CT, et al. (2011) A diverse range of gene products are effectors of the type I interferon antiviral response. Nature 472: 481-485.
76. Malakhova OA, Zhang DE (2008) ISG15 inhibits Nedd4 ubiquitin E3 activity and enhances the innate antiviral response. J Biol Chem 283: 8783-8787.
77. Vreede FT, Fodor E (2010) The role of the influenza virus RNA polymerase in host shut-off. Virulence 1: 436-439.
78. Amit I, Garber M, Chevrier N, Leite AP, Donner Y, et al. (2009) Unbiased reconstruction of a mammalian transcriptional network mediating pathogen responses. Science 326: 257-263.

79. Zhao B, Bower MJ, McDevitt PJ, Zhao H, Davis ST, et al. (2002) Structural basis for Chk1 inhibition by UCN-01. The Journal of biological chemistry 277: 46609-46615.
80. Jackson JR, Gilmartin A, Imburgia C, Winkler JD, Marshall LA, et al. (2000) An indolocarbazole inhibitor of human checkpoint kinase (Chk1) abrogates cell cycle arrest caused by DNA damage. Cancer research 60: 566-572.
81. Ramirez RD, Sheridan S, Girard L, Sato M, Kim Y, et al. (2004) Immortalization of human bronchial epithelial cells in the absence of viral oncoproteins. Cancer Res 64: 9027-9034.
82. Komurov K, White MA, Ram PT (2010) Use of data-biased random walks on graphs for the retrieval of context-specific networks from genomic data. PLoS Comput Biol 6.
83. Baron RA, Tavare R, Figueiredo AC, Blazewska KM, Kashemirov BA, et al. (2009) Phosphonocarboxylates inhibit the second geranylgeranyl addition by Rab geranylgeranyl transferase. The Journal of biological chemistry 284: 6861-6868.
84. Walsh KB, Teijaro JR, Wilker PR, Jatzek A, Fremgen DM, et al. (2011) Suppression of cytokine storm with a sphingosine analog provides protection against pathogenic influenza virus. Proc Natl Acad Sci U S A 108: 12018-12023.
85. Walsh KB, Teijaro JR, Rosen H, Oldstone MB (2011) Quelling the storm: utilization of sphingosine-1-phosphate receptor signaling to ameliorate influenza virus-induced cytokine storm. Immunol Res 51: 15-25.